symmetry

MDPI

Article

A Novel Weibull–Generalized Exponential Competing Risks Model: Statistical Inference, Bootstrap Validation, and Survival Prediction

Abdulrahman M. A. Aldawsari [1,*], Anas F. I. Alharshan [1], Aliyu Ismail Ishaq [2] and Abdullahi Ubale Usman [3]

[1] Department of Mathematics, College of Sciences and Humanities, Prince Sattam Bin Abdulaziz University, Al-Kharj 16273, Saudi Arabia; af.alharshan@psau.edu.sa
[2] Department of Statistics, Ahmadu Bello University, Zaria 810106, Nigeria; binishaq05@gmail.com
[3] Department of Statistics, Aliko Dangote University of Science and Technology, Wudil 713101, Nigeria; ubaleusman@kustwudil.edu.ng
* Correspondence: abd.aldawsari@psau.edu.sa

Abstract

Competing-risks survival data occur when an event can happen by various failure modes. The Weibull and generalized exponential distributions are popular distributions for survival and reliability studies, but they are not necessarily suitable for all complicated lifetime situations when they are employed as single distributions. A four-parameter Weibull–Generalized Exponential Competing Risks distribution is proposed, based on two independent latent failure times, each having a Weibull and generalized exponential distribution. The observed lifetime is the minimum of these lifetimes, and the resulting survival function is the product of the survival functions of the individual lifetimes, while the hazard function is the sum of the hazards of the individual lifetimes. Distributional and reliability properties of the model are explored and the parameters are estimated by the maximum likelihood method. A parametric bootstrap with 2000 replications evaluates the variability of estimation, confidence intervals and goodness of fit. WGECR gave the highest log-likelihood and the lowest information criteria, and had a Cox–Snell discrepancy of 0.2376 when applied to multiple myeloma survival data. The bootstrap goodness-of-fit test indicated a p-value of 0.0720, which is not significant at 5%. Moreover, a Hybrid Random Survival Forest (Hybrid RSF) was developed by incorporating the features of the survival probability from WGECR into the original covariates. It achieved a mean C-index of 0.8798, mean integrated Brier score of 0.0336 and time-dependent AUC of 0.8862 compared with 0.4286 of conventional RSF and 0.8697 of WGECR-RSF. The results validate the ability of WGECR to handle competing risks modeling and suggest distribution-informed features may be beneficial for survival prediction. The framework could serve as a tool for health care practitioners and planning agencies to make survival assessments and decisions.

Keywords: Weibull–generalized exponential competing risks; right-censored data; parametric bootstrap; Cox–Snell residuals; random survival forest; survival prediction.

Check for updates

Academic Editors: Jin-Ting Zhang and Tianming Zhu

Received: 5 October 2026
Revised: 3 November 2026
Accepted: 16 November 2026
Published: 25 November 2026

Copyright: © 2026 by the authors. Licensee MDPI, Basel, Switzerland. This article is an open access article distributed under the terms and conditions of the Creative Commons Attribution (CC BY) license.

1. Introduction

Survival analysis is an essential tool for the analysis of time-to-event data and has been applied in medical research, reliability engineering, epidemiology, and other areas where the time interval until some event of interest occurs is of interest, among others [1–3]. However, in many practical situations, an individual or system could be subjected to

multiple possible failure modes, one or more of which could occur first and obscure the occurrence of the other failure modes. These types of scenarios are often called competing-risks problems [4,5]. Analysis of competing risks is therefore not only interested in the distribution of the overall failure time, but also in the mechanisms by which the different causes give rise to the failure process observed [6].

The statistical analysis of competing risks has developed from early attempts to model alternative failure modes [7] via the development of cause-specific failure analysis and multiple-state models [4,8], to the important nonparametric approach for comparing cumulative incidence functions developed by [9]. Latent failure-time formulation: When the failure time is observed, it is the minimum of the competing failure times, and independence implies that the overall survival function is the product of the cause-specific survival functions and the cumulative hazard is the sum of the cause-specific cumulative hazards [8]. The parametric competing-risks models are appealing because of their tractable survival, hazard, and reliability functions and likelihood-based inference. Specifically, the Weibull distribution is still well known since it includes increasing, decreasing, and constant hazard rates, and in recent years, there has been research on the Weibull competing-risks models in the context of progressive and adaptive censoring schemes [10]. The Weibull distribution is widely used in lifetime analysis due to its simplicity, easy-to-interpret parameters, and the capability of modeling decreasing, constant, and increasing hazard rates [11]. However, it might not be able to describe more complicated or non-monotone failure patterns with its single shape parameter. The generalized exponential (GE) distribution, which is a novel distribution proposed by [12] and has been widely studied in lifetime and reliability analysis [13], offers greater flexibility by having an additional shape parameter. But each distribution represents one failure mechanism and can be limiting if other failure mechanisms have different lifetimes. In recent times, competing-risks models based on flexible Weibull and generalized distributions have also been explored [10,14].

Different lifetime distributions can be included in a competing-risks model, and each failure mechanism can be modeled separately based on its characteristics. Recently, some studies have been proposed, with generalizations of the model in the form of flexible formulations in generalized, hybrid, and multistate approaches, such as a generalized linear-exponential model, a bivariate exponentiated generalized inverted exponential model, and a generalized-family model as in [15–17]. The flexible lifetime formulations continue to be developed using Birnbaum–Saunders-based competing-risks models, and examples of the phase-type, parametric, and Bayesian models developed to address the challenges of heterogeneous failure mechanisms [18–20]. Other more recent reviews emphasize the need for flexible and computationally efficient techniques for competing-risks analysis [21,22]. These developments allow for the use of complementary lifetime distributions as a model for a variety of competing failure mechanisms without loss of convenient distributional and reliability features.

The Weibull and GE distributions are popular choices in the field of survival analysis and reliability engineering due to their mathematical properties and the ease of interpretation of their parameters. But for some complex lifetime data, their traditional shapes may prove to be inadequate. The Weibull distribution can model a hazard function with increasing, decreasing, and constant rates, but its standard specification might not provide enough flexibility to model more complicated non-monotonic hazard patterns. An alternative parametric model is the GE distribution, which has an extra shape parameter but may be insufficient to represent several competing failure modes with different lifetimes. In practical applications, such as medical life tests and reliability engineering, failure modes might have differing life characteristics. Using one distribution for these causes might then impose some restrictive assumptions on the failure process.

To overcome this limitation, we propose a four-parameter Weibull–generalized exponential competing-risks (WGECR) model by assuming that there are two independent latent failure times, T_1 and T_2, with Weibull and GE distributions, respectively. The observed lifetime is $T = \min(T_1, T_2)$, which is the time of the first failure event. This construction enables the two competing causes to exhibit unique distributional properties and still permits the use of a tractable framework to calculate survival, hazard, and reliability functions and to perform likelihood-based inference. The motivation for the Weibull–GE combination is the complementary attributes of these two established distributions and the ability to model a variety of competing failure mechanisms with an interpretable model. It is not as complex as other distributional constructions but provides a good trade-off between the flexibility of the model and the tractability of its analysis, with relative performance varying by both the data and the model. The proposed model is tested using maximum likelihood estimation, Monte Carlo simulation, goodness-of-fit comparisons, parametric bootstrap validation, and an application to multiple myeloma survival data.

The paper is organized in the following way: In Section 2, the proposed WGECR model is presented, and the basic distributional properties of this model are derived. A statistical and reliability characterization of the proposed model, including series representation, moments, mean time to failure, mean residual life, and numerical quantile function, is built in Section 3. Section 4 presents the methods of statistical inference and model validation, including maximum likelihood estimation, model selection criteria, validation of the Cox–Snell residual, and parametric bootstrap. The Cox–Snell residual analysis and parametric bootstrap are used to validate the WGECR model, with the survival data from multiple myeloma. In Section 5, the proposed Cox proportional hazards distribution-guided random survival forest (CoxPH-DRSF) model for survival prediction is introduced and tested for performance and compared with the traditional Cox proportional hazards model and random survival forest model. Finally, Section 6 summarizes this paper.

2. Construction of a New Hybrid Probability Distribution: Weibull–Generalized Exponential Competing-Risks Model

In this section, we propose a new hybrid probability distribution obtained by combining two independent latent failure times associated with different competing risk mechanisms. The motivation is to develop a flexible model that can capture complex failure patterns by merging the properties of two well-known distributions. Let T_1 and T_2 denote the latent failure times corresponding to two independent causes of failure. The observable failure time is defined as the minimum of these two latent times, i.e., $T = \min(T_1, T_2)$.

For the construction of the hybrid model, we assume that the first latent failure time T_1 follows a Weibull distribution, while the second latent failure time T_2 follows a generalized exponential distribution, with the assumption that T_1 and T_2 are statistically independent. We refer to this newly constructed hybrid distribution as the WGECR model. The parameter vector of the proposed WGECR distribution is given by $\boldsymbol{\eta} = (\beta, \theta, \alpha, \lambda)^T$, where $\beta, \theta, \alpha, \lambda > 0$.

To specify the WGECR distribution, we begin with the Weibull component. The cumulative hazard function for the Weibull component is defined as

$$H_1(t) = \beta t^{\theta}, \qquad t > 0, \tag{1}$$

where β is a scale parameter and θ is a shape parameter.

The probability of a component or a system surviving beyond time (t) is referred to as the survival function. The larger the value of the survival function at a given time, the higher the probability that the individual will still live at a later time. A lower value, on the other hand, means that the accumulated probability of the event is higher; that is, the event

has already happened more often. The survival function can be used in practice to assess the expected lifetimes of operational units and define the time scales that are significant to inspection, maintenance and replacement decisions.

Therefore, the survival function for the Weibull component is presented as

$$S_1(t) = \exp(-\beta t^{\theta}), \tag{2}$$

The second competing failure mechanism is assumed to be of the generalized exponential distribution. The cumulative hazard and survival functions are defined by

$$H_2(t) = -\log\left[1 - (1 - \exp(-\lambda t))^{\alpha}\right], \qquad t > 0, \tag{3}$$

and

$$S_2(t) = 1 - (1 - \exp(-\lambda t))^{\alpha}, \qquad t > 0, \tag{4}$$

where α is a shape parameter and λ is a scale parameter.

The proposed WGECR model cumulative hazard function is the sum of the component-specific cumulative hazard functions:

$$H(t) = H_1(t) + H_2(t) = \beta t^{\theta} - \log\left[1 - (1 - \exp(-\lambda t))^{\alpha}\right], \qquad t > 0. \tag{5}$$

In this case, the scale parameters are β and λ while the shape parameters are θ and α. The independence of the latent failure times leads automatically to the additive representation in (5).

The survival function is derived from $S(t) = \exp[-H(t)]$, which yields

$$S(t) = \exp(-\beta t^{\theta})\left[1 - (1 - \exp(-\lambda t))^{\alpha}\right]. \tag{6}$$

The function $F(t)$ is called the cumulative distribution function (CDF) because it gives the probability that the event of interest has occurred up to time t. Its reliability measurement from a reliability point of view is a direct measure of accumulated failure probability up to a given operating time. If the reliability requirement is for maximum acceptable probability of failure by some specific time, for instance, the estimated cumulative distribution function can be used to determine if the fitted model is in compliance with the requirement.

Therefore, based on (6), we determine the CDF of the proposed WGECR model

$$F(t) = 1 - \exp(-\beta t^{\theta})\left[1 - (1 - \exp(-\lambda t))^{\alpha}\right], \qquad t > 0. \tag{7}$$

If the unit is known to survive to t, then the hazard function is the rate at which the event occurs at t. It is a rate and not a probability of failure at a particular time. It provides information on the changes in the failure process through its time dynamics. If the hazard rate is increasing, then the failure rate will be larger at a later time than it was at an earlier time for the first time; if the hazard rate is decreasing, then the failure rate will be smaller at a later time than it was at an earlier time for the remaining units. A non-monotonic hazard rate could be due to the different stages of the failure process. The pattern that is associated with the WGECR model depends on the parameter values of the distribution and should not be assumed from the name and/or formulation of the distribution of the model.

Consequently, the hazard function of the proposed WGECR model is given by (6) as

$$h(t) = -\frac{d}{dt}\log S(t) = \beta\theta t^{\theta-1} + \frac{\alpha\lambda \exp(-\lambda t)(1 - \exp(-\lambda t))^{\alpha-1}}{1 - (1 - \exp(-\lambda t))^{\alpha}}, \qquad t > 0. \tag{8}$$

Finally, $f(t)$ is the probability density function (PDF) of the proposed WGECR model, which is obtained from (6) and (8) to get the density function, $f(t) = h(t)S(t)$. Therefore,

$$\begin{aligned} f(t) &= \exp(-\beta t^{\theta})\left[1-(1-\exp(-\lambda t))^{\alpha}\right]\left[\beta\theta t^{\theta-1} + \frac{\alpha\lambda\exp(-\lambda t)(1-\exp(-\lambda t))^{\alpha-1}}{1-(1-\exp(-\lambda t))^{\alpha}}\right] \\ &= \beta\theta t^{\theta-1}\exp(-\beta t^{\theta})\left[1-(1-\exp(-\lambda t))^{\alpha}\right] \\ &+ \alpha\lambda\exp(-\lambda t)(1-\exp(-\lambda t))^{\alpha-1}\exp(-\beta t^{\theta}), \qquad t>0. \end{aligned} \tag{9}$$

The PDF of event times provides information about the distribution of the event times and shows where failures are more concentrated. In the proposed WGECR distribution, it is a combination of the contributions from the Weibull and the generalized exponential failure mechanisms. For practical use, the PDF can assist in identifying periods in which failures are more likely, which can be used for maintenance scheduling, resource allocation, and reliability assessment.

2.1. Validity of the Proposed WGECR Model

The proposed WGECR is validated by checking its cumulative hazard function, survival function, CDF, PDF, and hazard function to ensure it satisfies the basic properties of a valid probability model.

Let $t > 0$ and $\lambda > 0$. This implies $0 < \exp(-\lambda t) < 1$, and hence $0 < 1-\exp(-\lambda t) < 1$. Since $\alpha > 0$, $0 < (1-\exp(-\lambda t))^{\alpha} < 1$, and $0 < 1-(1-\exp(-\lambda t))^{\alpha} < 1$, which implies $-\log\left[1-(1-\exp(-\lambda t))^{\alpha}\right] > 0$.

Since $\beta t^{\theta} > 0$, it follows from (5) that $H(t) > 0, t > 0$. Moreover,

$$\lim_{t\to 0^+} H(t) = 0.$$

As $t \to \infty$, $\beta t^{\theta} \to \infty$, while $1-(1-\exp(-\lambda t))^{\alpha} \to 0$. Hence,

$$\lim_{t\to\infty} H(t) = \infty.$$

In addition, $H'(t) = h(t)$, where $h(t)$ is as provided in (8). Both terms of $h(t)$ are non-negative for $t > 0$ so that $H'(t) \geq 0$ for $t > 0$. This means that $H(t)$ is nondecreasing and has the fundamental properties. A cumulative hazard function is a function that accumulates the hazards.

The survival function is related to the cumulative hazard, which is given by $S(t) = \exp[-H(t)]$. At the lower boundary,

$$\begin{aligned} \lim_{t\to 0^+} S(t) &= \lim_{t\to 0^+} \exp(-\beta t^{\theta})\left[1-(1-\exp(-\lambda t))^{\alpha}\right] \\ &= 1. \end{aligned}$$

At the upper boundary,

$$\begin{aligned} \lim_{t\to\infty} S(t) &= \lim_{t\to\infty} \exp(-\beta t^{\theta})\left[1-(1-\exp(-\lambda t))^{\alpha}\right] \\ &= 0. \end{aligned}$$

As $S'(t) \leq 0$ for all t, the survival function is nonincreasing. Thus, $S(t)$ is an acceptable survival function.

The validity of the cumulative distribution function is as follows:

$$\lim_{t\to 0^+} F(t) = 1 - \lim_{t\to 0^+} S(t) = 0,$$

and

$$\lim_{t\to\infty} F(t) = 1 - \lim_{t\to\infty} S(t) = 1.$$

Differentiate $F(t) \Rightarrow F'(t) = f(t)$. Because $f(t) \geq 0$ for $t > 0$, it follows that $F(t)$ is a nondecreasing function. Hence, $F(t)$ is a proper CDF.

We have

$$f(t) = \beta\theta t^{\theta-1}\exp(-\beta t^{\theta})\left[1-(1-\exp(-\lambda t))^{\alpha}\right] + \alpha\lambda\exp(-\lambda t)(1-\exp(-\lambda t))^{\alpha-1} \times \exp(-\beta t^{\theta}).$$

The integral

$$\int_0^{\infty} f(t)dt = F(\infty) - F(0^+) = 1 - 0 = 1.$$

So, $f(t)$ is a proper PDF.

From the above results, it follows that under the assumption that $\beta > 0$, $\theta > 0$, $\alpha > 0$ and $\lambda > 0$, the proposed WGECR model fulfills all fundamental requirements of a proper probability model. Thus, the WGECR is a proper four-parameter lifetime model.

2.2. Shape Behavior of the Proposed WGECR Model

The shape characteristics of the WGECR distribution are investigated through the asymptotic properties of its probability density function and hazard rate function. This analysis examines how the model parameters influence the behavior of these functions at the boundaries of the support, and identifies the various distributional and hazard rate shapes that the model can accommodate. Both the PDF and hazard function are discussed in detail in this section.

2.2.1. Shape Behavior of the PDF

The shape properties of the proposed model can be explored by the limiting behavior of its PDF provided in (9).

For $t \to 0^+$, we use $1-\exp(-\lambda t) \sim \lambda t$ and $\exp(-\beta t^{\theta}) \to 1$, and investigate the behavior of $f(t)$ as $t \to 0^+$. Consequently, $(1-\exp(-\lambda t))^{\alpha} \sim (\lambda t)^{\alpha}$, and hence

$$f(t) \sim \beta\theta t^{\theta-1} + \alpha\lambda^{\alpha} t^{\alpha-1}, \qquad t \to 0^+. \tag{10}$$

Hence, the behavior as $t \to 0$ of the density is dictated by the values of α and θ

$$\lim_{t\to 0^+} f(t) = \begin{cases} 0, & \alpha > 1,\ \theta > 1, \\ \lambda, & \alpha = 1,\ \theta > 1, \\ \beta, & \theta = 1,\ \alpha > 1, \\ \beta + \lambda, & \alpha = 1,\ \theta = 1, \\ \infty, & \alpha < 1 \text{ or } \theta < 1. \end{cases} \tag{11}$$

As t goes to ∞, then $\exp(-\lambda t) \to 0$ and $1-(1-\exp(-\lambda t))^{\alpha} \sim \alpha\exp(-\lambda t)$, for the right tail behavior. Therefore,

$$f(t) \sim \alpha\lambda\exp(-\lambda t) + \alpha\beta\theta t^{\theta-1}\exp\left(-\beta t^{\theta} - \lambda t\right), \qquad t \to \infty, \tag{12}$$

which gives

$$\lim_{t\to\infty} f(t) = 0. \tag{13}$$

The above limiting results give helpful information on the shape that the density may assume. The density has the property that $f(0^+) = 0$ and $f(\infty) = 0$ when $\alpha > 1$ and $\theta > 1$, and this corresponds to an interior mode. If $\alpha < 1$ or $\theta < 1$, the density is not finite at the origin and tends to zero for large t to the right, leading to a right-skewed and/or sharply peaked density.

2.2.2. Shape Behavior of the Hazard Function

The hazard function is the instantaneous failure rate at time t given that the object has not failed by time t. Recall that the hazard function of the proposed model is

$$h(t) = \beta\theta t^{\theta-1} + \frac{\alpha\lambda \exp(-\lambda t)(1-\exp(-\lambda t))^{\alpha-1}}{1-(1-\exp(-\lambda t))^{\alpha}} = A(t) + B(t),$$

where $A(t) = \beta\theta t^{\theta-1}$, and $B(t) = \frac{\alpha\lambda \exp(-\lambda t)(1-\exp(-\lambda t))^{\alpha-1}}{1-(1-\exp(-\lambda t))^{\alpha}}$.

The asymptotics of the hazard function as $t \to 0$ follow from the expansion $1 - \exp(-\lambda t) \sim \lambda t$. Hence,

$$h(t) \sim \beta\theta t^{\theta-1} + \alpha\lambda^{\alpha} t^{\alpha-1}. \tag{14}$$

Therefore,

$$\lim_{t\to 0^+} h(t) = \begin{cases} 0, & \alpha > 1,\ \theta > 1, \\ \lambda, & \alpha = 1,\ \theta > 1, \\ \beta, & \theta = 1,\ \alpha > 1, \\ \beta + \lambda, & \alpha = 1,\ \theta = 1, \\ \infty, & \alpha < 1 \text{ or } \theta < 1. \end{cases} \tag{15}$$

For the right tail, the second component of the hazard function is given by

$$\frac{\alpha\lambda \exp(-\lambda t)(1-\exp(-\lambda t))^{\alpha-1}}{1-(1-\exp(-\lambda t))^{\alpha}} \sim \lambda \exp(-\lambda t), \qquad t \to \infty.$$

Consequently,

$$h(t) \sim \beta\theta t^{\theta-1} + \lambda \exp(-\lambda t), \qquad t \to \infty, \tag{16}$$

and hence

$$\lim_{t\to\infty} h(t) = \begin{cases} \infty, & \theta > 1, \\ \beta, & \theta = 1, \\ 0, & 0 < \theta < 1. \end{cases} \tag{17}$$

The limiting results describe the boundary behavior of the hazard function, whereas the sign of $h'(t)$ determines its monotonicity and the location of any turning points. It is therefore essential to examine the sign of $h'(t)$ for different parameter combinations to establish whether the hazard function exhibits increasing, decreasing, bathtub, or modified bathtub shapes.

The relationship among parameter conditions, asymptotic behavior, and the resulting shapes of the proposed density and hazard functions is summarized in Table 1. The behavior of the density function at $t = 0$ and $t \to \infty$ explains the occurrence of various shapes, including unimodal, sharply peaked, bathtub-shaped, and right-skewed forms. Similarly, these boundary properties account for increasing, decreasing, constant, and bathtub-shaped hazard functions. These results highlight the flexibility of the proposed model in describing heterogeneous and censored survival data, such as those arising from multiple myeloma.

Table 1. Parameter conditions and possible shapes of the WGECR model.

Parameter Condition	PDF Shape	Hazard Shape
$\alpha > 1,\ \theta > 1$	Near-symmetric	Increasing
$\alpha = 1,\ \theta > 1$	Left-skewed	Increasing/non-monotone
$\alpha = \theta = 1$	Finite-origin density	Constant
$\alpha < 1,\ 0 < \theta < 1$	Right-skewed	Decreasing
$\alpha < 1,\ \theta > 1$	Unimodal	Bathtub
$\alpha \geq 1,\ \theta < 1$	Unimodal	Modified bathtub

The flexibility of the shape of the proposed model is illustrated by Figures 1 and 2, which confirm the summary in Table 1. As summarized in the table, the PDF adapts the reverse-J-shaped, modified unimodal, left-skewed, and near-symmetric shapes consistent with the parameter values and asymptotic behavior, while the hazard function adapts the decreasing, bathtub, modified bathtub, increasing, and approximately constant shapes for the same parameter values and asymptotic behavior. These results highlight the ability of the proposed model to account for significant variation in the concentration, skewness, modal location, tail behavior, and failure risk, making it suitable for various applications. A prominent application of such models is a multiple failure time dataset that is censored, represented by Myeloma data.

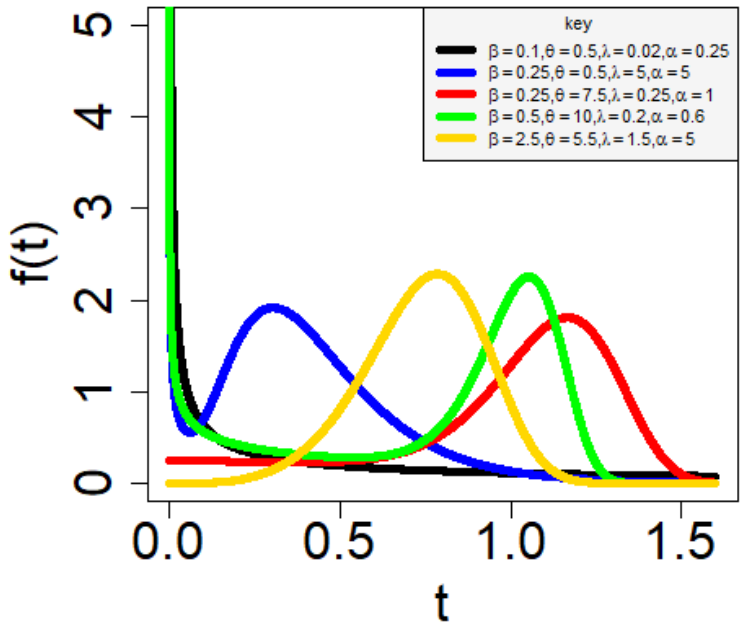


Figure 1. PDF shapes of the WGECR model for different parameter settings.

Figure 1 shows the flexibility of the proposed PDF with five different combinations of parameters. These combinations are chosen to illustrate the flexibility of the WGECR model to model various shapes of density, such as reverse-J-shaped, modified unimodal, left-skewed and approximately symmetric. In particular, the black curve (corresponding to $(\beta, \theta, \lambda, \alpha) = (0.1, 0.5, 0.02, 0.25)$) has a reverse-J shape; the density is high near the origin, and gets lower as time increases. This is typical behavior and the theory approximation in (10) implies that $f(t) \to \infty$ as $t \to 0^+$ when $0 < \theta < 1$ and $0 < \alpha < 1$. The density also tends to 0 as $t \to \infty$, which gives it a long right tail. The remaining combinations of parameters were chosen to show a range of different density shapes for various parameter combinations. These values are not used for model empirical parameter estimation, but simply for the representation in a graphical way, showing the flexibility of the proposed

model, which can describe various lifetime distributions. Similarly, the blue and green curves show modified unimodal distributions, where the curves have peaks at interior modes and decay at different rates. The difference is that the red curve is left-skewed with more numbers in the higher survival times, and the gold curve is more unimodal but is nearly symmetric in distribution, with more numbers in the middle survival time. The wide variety of these profiles suggests that the proposed model is flexible enough to capture a range of survival-time distributions that can exhibit different degrees of concentration, skewness, modal location, and tail behavior, particularly for the multiple myeloma survival data.

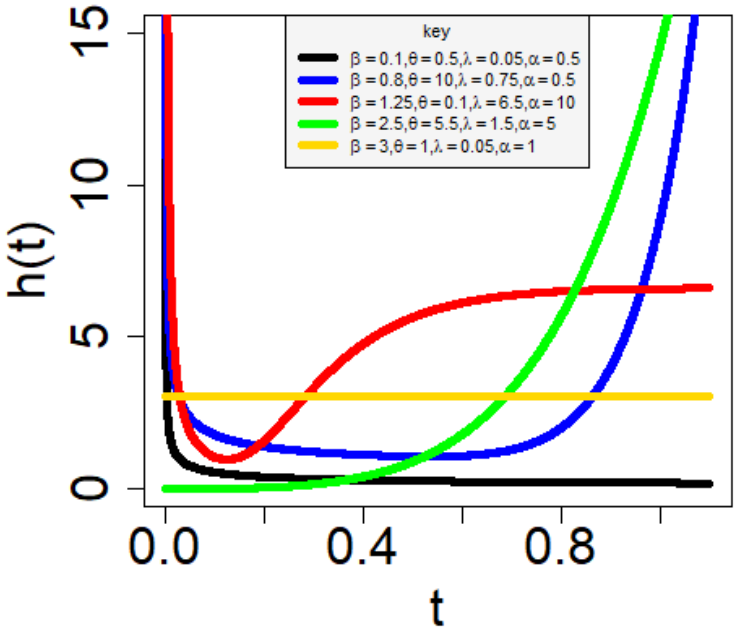


Figure 2. Hazard shapes of the WGECR model for different parameter settings.

The flexibility of the proposed hazard function is demonstrated in Figure 2 by five different combinations of the parameters. These combinations have been chosen to represent a variety of hazard-rate forms which the WGECR model is able to model, such as decreasing, bathtub-shaped, modified bathtub-shaped, increasing, and approximately constant hazards. The black curve, representing $(\beta, \theta, \lambda, \alpha) = (0.1, 0.5, 0.05, 0.5)$, has a decreasing hazard function, in particular. This selection is in line with the theory from this section: If $0 < \theta < 1$ and $0 < \alpha < 1$, then the hazard function becomes infinite as t tends to 0^+. All other combinations of the parameters were selected in order to show different hazard patterns for different combinations of parameters. The values are not estimates from the multiple myeloma dataset but are illustrative. The curves are shown together to illustrate the flexibility of this proposed model for the different failure-risk patterns over time. The blue curve $((\beta, \theta, \lambda, \alpha) = (0.5, 10, 0.75, 0.5))$ exhibits a clear "bathtub" shape in which the hazard first decreases and also reaches a minimum, but then starts to rise quickly again. This kind of behavior is an important type of lifetime data with an initial risk and a relatively short time to reach a minimum, followed by an increasing risk of survival times. The modified bathtub behavior, indicated by the red curve, has $(\beta, \theta, \lambda, \alpha) = (1.25, 0.1, 6.5, 10)$, where the hazard starts off high, then decreases rapidly, and only turns higher again at the end to a finite level. The late-time hazard can grow and not diverge, which is a good pattern to use in this situation. The green curve is clear of any decrease in hazard, with a chance of failure that gradually rises over time, beginning near zero and rising quickly over time. Lastly, the gold curve has a hazard similar to a constant for the range of data used,

with values close to 3 and suggesting a rather constant failure risk over time. In general, the contrasting patterns reveal that the proposed model can cover a wide range of hazard rate patterns from decreasing to bathtub, bathtub to increasing and bathtub to approximately constant hazards. Flexibility such as this is especially important for heterogeneous survival data, such as multiple myeloma data, where the hazard of death could differ significantly during different periods of follow-up.

3. Statistical Features of the WGECR Model

The statistical and reliability properties of the proposed WGECR model are discussed in this section. The PDF and the survival functions are represented as series, and then the raw moments are produced. The important reliability measures, namely the mean time to failure and the mean residual life, are also derived to describe the lifetime that is expected and remains. Finally, the quantile function is discussed, and the numerical estimation of quantiles using the Newton–Raphson method is discussed.

3.1. Series Expansion of the WGECR Model

The series solution of the WGECR model gives analytical expressions for its PDF and survival function that are useful for analysis. The distributional components can be expressed as convergent series, thereby allowing for convenient derivation of several important statistical properties.

3.1.1. Series Expansion of the PDF

Consider the PDF in (9) for $t > 0$. Let $z = e^{-\lambda t}$, where $0 < z < 1$. Apply the generalized binomial expansion to get the following:

$$(1-z)^{\alpha} = \sum_{k=0}^{\infty} (-1)^k \binom{\alpha}{k} z^k,$$

and hence

$$1-(1-z)^{\alpha} = \sum_{k=1}^{\infty} (-1)^{k+1} \binom{\alpha}{k} z^k. \tag{18}$$

Similarly,

$$(1-z)^{\alpha-1} = \sum_{k=0}^{\infty} (-1)^k \binom{\alpha-1}{k} z^k. \tag{19}$$

Substituting (18) and (19) into (9), we get

$$\begin{aligned} f(t) = \beta\theta t^{\theta-1} e^{-\beta t^{\theta}} \sum_{k=1}^{\infty} (-1)^{k+1} \binom{\alpha}{k} e^{-k\lambda t} \\ + \alpha\lambda e^{-\beta t^{\theta}} \sum_{k=0}^{\infty} (-1)^k \binom{\alpha-1}{k} e^{-(k+1)\lambda t}. \end{aligned} \tag{20}$$

Using the Taylor expansions

$$e^{-k\lambda t} = \sum_{j=0}^{\infty} \frac{(-k\lambda t)^j}{j!}, \tag{21}$$

and

$$e^{-(k+1)\lambda t} = \sum_{j=0}^{\infty} \frac{[-(k+1)\lambda t]^j}{j!}, \tag{22}$$

we obtain

$$f(t) = \beta\theta e^{-\beta t^\theta} \sum_{k=1}^{\infty}\sum_{j=0}^{\infty}(-1)^{k+j+1}\binom{\alpha}{k}\frac{(k\lambda)^j}{j!}t^{\theta+j-1} + \alpha\lambda e^{-\beta t^\theta} \sum_{k=0}^{\infty}\sum_{j=0}^{\infty}(-1)^{k+j}\binom{\alpha-1}{k}\frac{[(k+1)\lambda]^j}{j!}t^j. \tag{23}$$

For convenience, define

$$\psi_{k,j} = \beta\theta(-1)^{k+j+1}\binom{\alpha}{k}\frac{(k\lambda)^j}{j!}, \qquad k \geq 1,\ j \geq 0,$$

and

$$\omega_{k,j} = \alpha\lambda(-1)^{k+j}\binom{\alpha-1}{k}\frac{[(k+1)\lambda]^j}{j!}, \qquad k \geq 0,\ j \geq 0.$$

Therefore, the PDF in (23) has the following series representation:

$$f(t) = e^{-\beta t^\theta}\left[\sum_{k=1}^{\infty}\sum_{j=0}^{\infty}\psi_{k,j}t^{\theta+j-1} + \sum_{k=0}^{\infty}\sum_{j=0}^{\infty}\omega_{k,j}t^j\right], \qquad t > 0. \tag{24}$$

3.1.2. Series Expansion of the Survival Function

The survival function in (6) may be written in terms of the generalized binomial expansion as in (18) with $z = e^{-\lambda t}$, where $0 < z < 1$.

$$S(t) = e^{-\beta t^\theta}\sum_{k=1}^{\infty}(-1)^{k+1}\binom{\alpha}{k}e^{-k\lambda t}. \tag{25}$$

Using the Taylor expansion in (21), equation (25) can be further expressed as

$$S(t) = e^{-\beta t^\theta}\sum_{k=1}^{\infty}\sum_{j=0}^{\infty}(-1)^{k+j+1}\binom{\alpha}{k}\frac{(k\lambda)^j}{j!}t^j. \tag{26}$$

3.2. Moments

The moments of the proposed WGECR model give useful measures of the central tendency and dispersion of the model. Suppose T is a random variable that has the proposed model. The rth raw moment of T exists if T exists, and is equal to

$$\mu'_r = \int_0^\infty t^r f(t)\,dt, \qquad r > 0. \tag{27}$$

The rth raw moment can be expressed by substituting the series representation of the PDF in (24) into (27) as follows:

$$\mu'_r = \sum_{k=1}^{\infty}\sum_{j=0}^{\infty}\psi_{k,j}\int_0^\infty t^{r+\theta+j-1}e^{-\beta t^\theta}\,dt + \sum_{k=0}^{\infty}\sum_{j=0}^{\infty}\omega_{k,j}\int_0^\infty t^{r+j}e^{-\beta t^\theta}\,dt. \tag{28}$$

If $q > 0$, then use the following identity to evaluate the integrals:

$$\int_0^\infty t^{q-1}e^{-\beta t^\theta}\,dt = \frac{1}{\theta}\beta^{-q/\theta}\Gamma\left(\frac{q}{\theta}\right), \tag{29}$$

where $\Gamma(\cdot)$ is the gamma function.

As in (28), consider $q = r + \theta + j$ for the first integral. Thus,

$$\int_0^\infty t^{r+\theta+j-1} e^{-\beta t^\theta}\, dt = \frac{1}{\theta}\beta^{-(r+\theta+j)/\theta}\Gamma\left(\frac{r+\theta+j}{\theta}\right). \tag{30}$$

In the second integral, let $q = r + j + 1$, so that

$$\int_0^\infty t^{r+j} e^{-\beta t^\theta}\, dt = \frac{1}{\theta}\beta^{-(r+j+1)/\theta}\Gamma\left(\frac{r+j+1}{\theta}\right). \tag{31}$$

After substituting (30) and (31) into (28), the following expression for the rth raw moment is obtained:

$$\begin{aligned}\mu'_r = {} & \frac{1}{\theta}\sum_{k=1}^{\infty}\sum_{j=0}^{\infty}\psi_{k,j}\beta^{-(r+\theta+j)/\theta}\Gamma\left(\frac{r+\theta+j}{\theta}\right) \\ & + \frac{1}{\theta}\sum_{k=0}^{\infty}\sum_{j=0}^{\infty}\omega_{k,j}\beta^{-(r+j+1)/\theta}\Gamma\left(\frac{r+j+1}{\theta}\right).\end{aligned} \tag{32}$$

The mean is obtained by setting $r = 1$ in (32), while the second raw moment is obtained by setting $r = 2$. The variance is then

$$\mathrm{Var}(T) = \mu'_2 - (\mu'_1)^2. \tag{33}$$

Higher-order moments, when finite, can be used to calculate measures such as skewness and kurtosis.

3.3. Moment Generating Function

The moment generating function (MGF) is a useful statistical function for summarizing a probability distribution and calculating the moments of the distribution, when it exists. Suppose T is a non-negative continuous random variable with the proposed WGECR distribution, and its PDF is denoted as $f(t)$. The MGF of T is given by

$$M_T(s) = \int_0^\infty e^{st} f(t)\, dt, \tag{34}$$

where $s \in \mathbb{R}$ is a parameter for which the expectation exists and where the integral is finite.

Consider the Taylor series expansion

$$e^{st} = \sum_{r=0}^{\infty}\frac{s^r t^r}{r!}. \tag{35}$$

The MGF can be expressed as

$$\begin{aligned}M_T(s) &= \int_0^\infty \left(\sum_{r=0}^{\infty}\frac{s^r t^r}{r!}\right) f(t)dt \\ &= \sum_{r=0}^{\infty}\frac{s^r}{r!}\int_0^\infty t^r f(t)dt \\ &= \sum_{r=0}^{\infty}\frac{\mu'_r}{r!}s^r,\end{aligned} \tag{36}$$

where μ'_r is the r-th raw moment.

Putting the raw-moment expression into (36), we receive

$$M_T(s) = \frac{1}{\theta}\sum_{r=0}^{\infty}\frac{s^r}{r!}\left[\sum_{k=1}^{\infty}\sum_{j=0}^{\infty}\psi_{k,j}\,\beta^{-(r+\theta+j)/\theta}\Gamma\left(\frac{r+\theta+j}{\theta}\right) + \sum_{k=0}^{\infty}\sum_{j=0}^{\infty}\omega_{k,j}\,\beta^{-(r+j+1)/\theta}\Gamma\left(\frac{r+j+1}{\theta}\right)\right]. \tag{37}$$

When $\theta > 1$, the MGF exists for all real numbers s.

3.4. Mean Time to Failure

The mean time to failure (MTTF) is an important reliability measure that quantifies the expected lifetime of a unit before failure. So, the MTTF for a non-negative continuous lifetime random variable T is defined as

$$\text{MTTF} = \int_0^{\infty} S(t)\,dt. \tag{38}$$

The survival function in (6) is used to find the MTTF of the proposed WGECR model given by

$$\text{MTTF} = \int_0^{\infty} \exp(-\beta t^{\theta})\left[1-(1-\exp(-\lambda t))^{\alpha}\right]dt. \tag{39}$$

The MTTF can also be written as a series expansion using the series representation in (26):

$$\text{MTTF} = \sum_{k=1}^{\infty}\sum_{j=0}^{\infty}(-1)^{k+j+1}\binom{\alpha}{k}\frac{(k\lambda)^j}{j!}\int_0^{\infty} t^j e^{-\beta t^{\theta}}dt. \tag{40}$$

Using the transformation $u = \beta t^{\theta}$, we have $\int_0^{\infty} t^j e^{-\beta t^{\theta}}dt = \frac{1}{\theta}\beta^{-\frac{j+1}{\theta}}\Gamma\left(\frac{j+1}{\theta}\right)$. Therefore, the series representation is included in the MTTF.

$$\text{MTTF} = \frac{1}{\theta}\sum_{k=1}^{\infty}\sum_{j=0}^{\infty}(-1)^{k+j+1}\binom{\alpha}{k}\frac{(k\lambda)^j}{j!}\beta^{-\frac{j+1}{\theta}}\Gamma\left(\frac{j+1}{\theta}\right). \tag{41}$$

The MTTF of the WGECR model is provided in (41) and can be used to delve into the effects of the model parameters on the expected lifetime.

3.5. Mean Residual Life

An important reliability measure is the mean residual life (MRL), which measures the expected remaining life of a unit that has survived up to time t. Given a non-negative continuous random variable T, the MRL function is defined as

$$m(t) = \frac{1}{S(t)}\int_t^{\infty} S(x)\,dx, \tag{42}$$

where $S(t)$ is the survival function of the proposed model. The MRL function of the proposed WGECR model is obtained by substituting the survival function of (6) into (42) as follows:

$$m(t) = \frac{\int_t^{\infty}\exp(-\beta x^{\theta})\left[1-(1-\exp(-\lambda x))^{\alpha}\right]dx}{\exp(-\beta t^{\theta})\left[1-(1-\exp(-\lambda t))^{\alpha}\right]}. \tag{43}$$

Using the series representation in (25), the numerator of (43) can be written as

$$\int_t^\infty S(x)\,dx = \sum_{k=1}^{\infty}(-1)^{k+1}\binom{\alpha}{k}\int_t^\infty \exp(-\beta x^\theta - k\lambda x)\,dx.$$

Thus, the MRL function can also be written as

$$m(t) = \frac{\sum_{k=1}^{\infty}(-1)^{k+1}\binom{\alpha}{k}\int_t^\infty \exp(-\beta x^\theta - k\lambda x)\,dx}{\exp(-\beta t^\theta)\left[1-(1-\exp(-\lambda t))^\alpha\right]}. \tag{44}$$

In particular, at $t = 0$, the MRL becomes the mean time to failure $m(0) = \text{MTTF}$. The function (43) can be numerically evaluated to determine the remaining useful life of a remaining unit.

3.6. Order Statistic

Suppose that $T_1, \ldots, T_n$ is an independent and identically distributed random sample from a continuous distribution whose CDF is $F(t)$ and the PDF is $f(t)$. Let the ith order statistic be $T_{(i)}$, the ith smallest observation in the sample. The PDF of $T_{(i)}$ is given by

$$f_{T_{(i)}}(t) = \frac{n!f(t)}{(i-1)!(n-i)!}[F(t)]^{i-1}[1-F(t)]^{n-i}, \qquad t>0, \qquad i=1,2,\ldots,n. \tag{45}$$

Applying the generalized binomial expansion of (19) to the last term on the right-hand side of (45) yields

$$f_{T_{(i)}}(t) = \frac{n!f(t)}{(i-1)!(n-i)!}\sum_{k_1=0}^{n-i}(-1)^{k_1}\binom{n-i}{k_1}[F(t)]^{i+k_1-1}, \qquad t>0. \tag{46}$$

Replacing the CDF of the proposed WGECR distribution in (46), we get

$$\begin{aligned} f_{T_{(i)}}(t) = {} & \frac{n!f(t)}{(i-1)!(n-i)!}\sum_{k_1=0}^{n-i}(-1)^{k_1}\binom{n-i}{k_1} \\ & \times\left[1-e^{-\beta t^\theta}\left\{1-\left(1-e^{-\lambda t}\right)^\alpha\right\}\right]^{i+k_1-1}. \end{aligned} \tag{47}$$

Expanding the last term again by the binomial theorem, we obtain

$$\begin{aligned} f_{T_{(i)}}(t) = {} & \frac{n!f(t)}{(i-1)!(n-i)!}\sum_{k_1=0}^{n-i}\sum_{k_2=0}^{i+k_1-1}(-1)^{k_1+k_2} \\ & \times\binom{n-i}{k_1}\binom{i+k_1-1}{k_2}e^{-k_2\beta t^\theta} \\ & \times\left[1-\left(1-e^{-\lambda t}\right)^\alpha\right]^{k_2}. \end{aligned} \tag{48}$$

Define

$$\Psi_{k_1,k_2} = \frac{n!}{(i-1)!(n-i)!}(-1)^{k_1+k_2}\binom{n-i}{k_1}\binom{i+k_1-1}{k_2}. \tag{49}$$

Consequently, the PDF of the ith order statistic, $T_{(i)}$, can be given by

$$f_{T_{(i)}}(t) = f(t)\sum_{k_1=0}^{n-i}\sum_{k_2=0}^{i+k_1-1}\Psi_{k_1,k_2}e^{-k_2\beta t^\theta}\left[1-\left(1-e^{-\lambda t}\right)^\alpha\right]^{k_2}. \tag{50}$$

Finally, substituting the WGECR PDF from (9) into (50), we obtain the PDF of the ith order statistic as

$$f_{T_{(i)}}(t) = \sum_{k_1=0}^{n-i} \sum_{k_2=0}^{i+k_1-1} \Psi_{k_1,k_2} e^{-k_2\beta t^\theta} \left[1-\left(1-e^{-\lambda t}\right)^\alpha\right]^{k_2} \times \left\{\beta\theta t^{\theta-1} e^{-\beta t^\theta}\left[1-\left(1-e^{-\lambda t}\right)^\alpha\right] + \alpha\lambda e^{-\lambda t}\left(1-e^{-\lambda t}\right)^{\alpha-1} e^{-\beta t^\theta}\right\}, \qquad t>0. \tag{51}$$

3.7. Identifiability Analysis

Identifiability is an essential characteristic of parametric statistical models which guarantees that the probability distribution of the model is completely defined by the parameters. A parametric model is globally identifiable if two distribution vectors that are equal under the model imply that their parameter vectors are equal.

Suppose that T is a non-negative random variable, whose distribution is assumed to be of the WGECR model with parameter vector $\boldsymbol{\eta} = (\beta, \theta, \lambda, \alpha) \in \Omega$ with $\Omega = (0, \infty)^4$. The survival function is given by

$$S(t;\boldsymbol{\eta}) = e^{-\beta t^\theta}\left[1-\left(1-e^{-\lambda t}\right)^\alpha\right], \qquad t>0.$$

The model is globally identifiable on Ω if

$$S(t;\boldsymbol{\eta}_1) = S(t;\boldsymbol{\eta}_2), \qquad \text{for all } t>0. \tag{52}$$

For all $\boldsymbol{\eta}_1,\ \boldsymbol{\eta}_2 \in \Omega$, it implies $\boldsymbol{\eta}_1 = \boldsymbol{\eta}_2$.

For an analysis of this condition, explore the restrictions of the parameters, namely $\theta = 1$ and $\alpha = 1$. In the following, under the restrictions, the survival function simplifies to

$$\begin{aligned} S(t;\beta,1,\lambda,1) &= e^{-\beta t}\left[1-\left(1-e^{-\lambda t}\right)\right] \\ &= e^{-\beta t} e^{-\lambda t} \\ &= e^{-(\beta+\lambda)t}, \qquad t>0. \end{aligned} \tag{53}$$

From this expression, it can be seen that on the subspace defined by $\theta = \alpha = 1$, the distribution is only a function of the sum of β and λ (namely, $(\beta+\lambda)$). As a result, the survival functions are the same for different pairs of positive parameters that add up to the same value.

For instance, take the two vectors of parameters

$$\begin{aligned} \boldsymbol{\eta}_1 &= (1,1,2,1), \\ \boldsymbol{\eta}_2 &= (2,1,1,1). \end{aligned}$$

Although $\boldsymbol{\eta}_1 \neq \boldsymbol{\eta}_2$, their corresponding survival functions satisfy

$$S(t;\boldsymbol{\eta}_1) = e^{-3t} = S(t;\boldsymbol{\eta}_2), \qquad t>0.$$

So, these different parameter vectors result in the same probability distribution. The CDFs of these are the same, for $(F(t;\boldsymbol{\eta}) = 1 - S(t;\boldsymbol{\eta}))$. Also, their PDFs are the same since they are computed by differentiating the same CDF.

From this, it follows that the mapping from the parameter vector to the induced probability distribution is not a one-to-one mapping. Therefore, the distribution of the WGECR cannot be identified globally on the whole parameter space $\Omega = (0, \infty)^4$. This is an automatic consequence of the explicit counterexample and shows that parameters cannot be uniquely determined in all of the parameter space from the probability distribution.

The non-identifiability result has important implications for parameter estimation and statistical inference. If $\theta = \alpha = 1$, then only the total quantity $(\beta + \lambda)$ can be identified and β and λ cannot be uniquely estimated. This structural ambiguity could impede numerical optimization, parameter interpretation and estimation of standard error. The analysis is done on this subspace, but it does not imply identifiability on another subspace; this other subspace would have to be proven separately mathematically. When using the proposed WGECR distribution, this constraint should be taken into account when interpreting the parameter estimates and evaluating the inferential properties of the distribution.

3.8. Quantile Function

The quantile function is a useful function for describing the distribution of a continuous random variable. It is convenient for computing the median, quartiles, and percentiles, for generating random variates, and for simulation studies. The u-th quantile of a continuous random variable T with cumulative distribution function $F(t)$ is the value $Q(u), 0 < u < 1$, such that

$$F(Q(u)) = u. \tag{54}$$

The CDF for the proposed model is given in (6). Setting $F(t) = u$ gives

$$1 - u = \exp\left(-\beta t^{\theta}\right)\left[1 - (1 - \exp(-\lambda t))^{\alpha}\right]. \tag{55}$$

When we take the natural logarithm, we get

$$\log(1 - u) = -\beta t^{\theta} + \log\left[1 - (1 - \exp(-\lambda t))^{\alpha}\right]. \tag{56}$$

Thus, the u-th quantile $Q(u)$ is the positive solution of

$$\beta Q(u)^{\theta} - \log\left[1 - (1 - \exp(-\lambda Q(u)))^{\alpha}\right] + \log(1 - u) = 0. \tag{57}$$

Because $Q(u)$ appears in both the power and the exponential, it is generally not possible to obtain a closed-form expression for it. So, it is necessary to use numerical methods to find the quantiles.

The quantile function of the proposed WGECR model is numerically solved by using the Newton–Raphson method. The quantile equation does not have a closed-form solution, so the method yields a convenient iterative algorithm for finding t that corresponds to a given cumulative probability u. A suitable initial approximation is calculated, and then successive estimates are computed by the Newton–Raphson iteration until a desired level of convergence is reached. This numerical method enables the estimation of the quantiles of the proposed model precisely, and it is especially useful for simulation as well as for reliability analysis.

The numerical quantiles of the proposed WGECR model are numerically calculated by using the Newton–Raphson procedure briefly described below in Algorithm 1:

Algorithm 1 Newton–Raphson method for computing $Q(u)$

Require: $u \in (0,1)$, $\alpha, \beta, \lambda, \theta > 0$, $t_0 > 0$, $\varepsilon = 10^{-8}$.
Ensure: Numerical estimate of $Q(u)$.
Define

$$g(t) = 1 - \exp(-\beta t^{\theta})\left[1 - (1 - \exp(-\lambda t))^{\alpha}\right] - u.$$

Define

$$g'(t) = \exp(-\beta t^{\theta})\left[\beta\theta t^{\theta-1}\left\{1 - (1 - \exp(-\lambda t))^{\alpha}\right\} + \alpha\lambda \exp(-\lambda t)(1 - \exp(-\lambda t))^{\alpha-1}\right].$$

Set $k = 0$.
repeat
Compute

$$t_{k+1} = t_k - \frac{g(t_k)}{g'(t_k)}.$$

Set $k \leftarrow k + 1$.
until $|t_k - t_{k-1}| < 10^{-8}$.
Set $Q(u) = t_k$.
return $Q(u)$.

The value of $Q(u)$ is the numerical estimate of the u-th quantile. In particular, $Q(0.25)$, $Q(0.50)$, and $Q(0.75)$ represent the first, median, and third quartiles, respectively.

The Newton–Raphson numerical technique was used to estimate the quantile function of the WGECR model at three selected probability levels $u = 0.25, u = 0.50, u = 0.75$, which correspond to the first, second and third quartiles, respectively. The numerical evaluation was made for the following parameter values: $\beta = 0.1, \theta = 0.5, \lambda = 0.02, \alpha = 0.25$ and starting value $t_0 = 0.5$. The iterative method was used by solving $F(t) = u$, until the absolute error between two successive estimates was sufficiently small. The resulting Newton–Raphson convergence processes are shown in Tables 2–4 respectively.

Table 2. Newton–Raphson iterations for estimating the $Q(0.25)$ with $\beta = 0.1, \theta = 0.5, \lambda = 0.02$, and $\alpha = 0.25$.

Iteration	t_k	$F(t_k)$	$g(t_k)$	$g'(t_k)$	t_{k+1}	Error
1	0.5000	0.3625	1.125×10^{-1}	0.1915	0.2500	2.500×10^{-1}
2	0.2500	0.3016	5.156×10^{-2}	0.3220	0.0899	1.601×10^{-1}
3	0.0899	0.2293	-2.068×10^{-2}	0.6837	0.1201	3.025×10^{-2}
4	0.1201	0.2479	-2.143×10^{-3}	0.5529	0.1240	3.877×10^{-3}
5	0.1240	0.2500	-2.490×10^{-5}	0.5401	0.1241	4.611×10^{-5}
6	0.1241	0.2500	-3.396×10^{-9}	0.5400	0.1241	6.289×10^{-9}

Table 3. Newton–Raphson iterations for estimating the $Q(0.50)$ with $\beta = 0.1, \theta = 0.5, \lambda = 0.02$, and $\alpha = 0.25$.

Iteration	t_k	$F(t_k)$	$g(t_k)$	$g'(t_k)$	t_{k+1}	Error
1	0.5000	0.3625	-1.375×10^{-1}	0.1915	1.2180	7.179×10^{-1}
2	1.2180	0.4572	-4.281×10^{-2}	0.0961	1.6630	4.454×10^{-1}
3	1.6630	0.4948	-5.161×10^{-3}	0.0749	1.7320	6.895×10^{-2}
4	1.7320	0.4999	-8.485×10^{-5}	0.0724	1.7330	1.172×10^{-3}
5	1.7330	0.5000	-2.337×10^{-8}	0.0724	1.7330	3.229×10^{-7}
6	1.7330	0.5000	-1.998×10^{-15}	0.0724	1.7330	2.753×10^{-14}

Table 4. Newton–Raphson iterations for estimating the $Q(0.75)$ with $\beta = 0.1, \theta = 0.5, \lambda = 0.02$, and $\alpha = 0.25$.

Iteration	t_k	$F(t_k)$	$g(t_k)$	$g'(t_k)$	t_{k+1}	Error
1	0.5000	0.3625	-3.875×10^{-1}	0.1915	2.5240	2.024×10^{0}
2	2.5240	0.5487	-2.013×10^{-1}	0.0530	6.3200	3.797×10^{0}
3	6.3200	0.6788	-7.118×10^{-2}	0.0233	9.3710	3.051×10^{0}
4	9.3710	0.7371	-1.288×10^{-2}	0.0158	10.1880	8.161×10^{-1}
5	10.1880	0.7494	-5.505×10^{-4}	0.0145	10.2260	3.807×10^{-2}
6	10.2260	0.7500	-1.080×10^{-6}	0.0144	10.2260	7.500×10^{-5}
7	10.2260	0.7500	-4.174×10^{-12}	0.0144	10.2260	2.898×10^{-10}

From the Newton–Raphson results, it was found that the values have converged successfully and quickly to the first quartile $Q(0.25)$, as shown in Table 2. If the initial value is $t_0 = 0.5$, then the first iteration is $F(t_0) = 0.3625$ and $g(t_0) = F(t_0) - 0.25 = 0.1125 > 0$. Thus, the estimate goes down to $t_1 = 0.2500$ in the Newton–Raphson update. In the second iteration, $F(t_1) = 0.3016$ and $g(t_1) = 0.0516 > 0$, resulting in a further reduction to $t_2 = 0.0899$. The algorithm slightly overshoots the target probability, with $F(t_2) = 0.2293$ and $g(t_2) = -0.02068 < 0$ at this stage. In subsequent calculations, the overshoot is taken care of, and the estimates are readjusted and converge to $0.1201, 0.1240, 0.1241$. The next few iterations correct for this overshoot, with estimates rising to $0.1201, 0.1240$ and finally 0.1241. The absolute error after each iteration starts at 2.50×10^{-1} and gradually reduces to 6.29×10^{-9}, which meets the convergence requirement. The numerical solution is checked to be a solution of $F(Q(0.25)) = 0.25$ at the point of convergence, $Q(0.25) \approx 0.1241$ and $F(0.1241) \approx 0.25$. Hence, the first quartile is approximately equal to $Q(0.25) \approx 0.1241$. The result shows that about 25% of the probability mass of the proposed distribution is below a survival time of about 0.1241 for the proposed model under the parameter setting $\beta = 0.1, \theta = 0.5, \lambda = 0.02$, and $\alpha = 0.25$.

The Newton–Raphson procedure to compute the median $Q(0.50)$ is employed and is found to converge to the true median for the parameter conditions $\beta = 0.1, \theta = 0.5, \lambda = 0.02$, and $\alpha = 0.25$, as presented in Table 3. Starting from the initial value $t_0 = 0.5$, the first iteration gives $F(t_0) = 0.3625$ and $g(t_0) = -0.1375 < 0$. The Newton–Raphson update then makes the estimation of t_1 more accurate, to $t_1 = 1.2180$. In the second iteration, $F(t_1) = 0.4572$ and $g(t_1) = -0.04281$, resulting in a further increase to $t_2 = 1.6630$. The next few iterations gradually get closer and closer to $u = 0.50$ and continue to close in on the estimate 1.7330. The convergence after the 3rd iteration is even more rapid. The absolute error decreases from 6.895×10^{-2} at the third iteration to 1.172×10^{-3}, 3.229×10^{-7}, and finally 2.753×10^{-14}. At the sixth iteration, $F(t) = 0.5000$ and $g(t) = -1.998 \times 10^{-15}$, which is effectively zero. To the accuracy obtained, the equation $F(Q(0.50)) = 0.50$ is satisfied, and the estimated median is $Q(0.50) \approx 1.7330$. This outcome suggests that under the given parameters, around 50% of the probability mass of the proposed distribution is below a survival time of around 1.7330. The following Newton–Raphson increments are all positive because the initial value $t_0 = 0.5$ has an accumulated probability that is below the desired mean probability, so that larger values of t will have to be used to reach the desired value of $F(t) = 0.50$.

The Newton–Raphson procedure is shown to be a successful method for estimating the third quartile, $Q(0.75)$, with the parameter setting $\beta = 0.1, \theta = 0.5, \lambda = 0.02$, and $\alpha = 0.25$, as provided in Table 4. Starting from the initial value $t_0 = 0.5$, the first iteration gives $F(t_0) = 0.3625$ and $g(t_0) = -0.3875 < 0$. The calculated cumulative probability is significantly less than the desired cumulative probability, so the Newton–Raphson update results in a significant increase in the estimate and gives $t_1 = 2.5240$. In the second iteration, $F(t_1) = 0.5487$ and $g(t_1) = -0.2013$, resulting in a further increase to $t_2 = 6.3200$. The next

iterations continue to make the distance between $F(t)$ and the specified value $u = 0.75$ smaller and smaller. The estimates are then raised to 9.3710, 10.1880, and 10.2260, and then the algorithm quickly enters the convergence phase. The absolute error decreases from 2.0240 in the first iteration to 3.7970, 3.0510, 0.8161, 0.03807, 7.500×10^{-5}, and finally 2.898×10^{-10}. At the seventh iteration, $F(t) = 0.7500$ and $g(t) = -4.174 \times 10^{-12}$, which is effectively zero. Hence, the estimated third quartile is $Q(0.75) \approx 10.2260$. Therefore, about 75% of the probabilities of the proposed distribution fall below a survival time of about 10.2260 with the given set of parameters. It is also observed that the value of $Q(0.75)$ is much larger than those of $Q(0.25)$ and $Q(0.50)$, which also suggests the extended right-tail behavior of the distribution for $\beta = 0.1, \theta = 0.5, \lambda = 0.02$, and $\alpha = 0.25$.

4. Statistical Inference and Model Validation

The validation and statistical inference procedure for the proposed WGECR model under right-censored data is presented in this section. Maximum likelihood estimation (MLE) is used to estimate the model parameters and the estimates are computed using numerical optimization. The model adequacy is assessed using likelihood-based criteria, information criteria, Cox–Snell residuals, and Kaplan–Meier comparisons. A parametric bootstrap is additionally used to assess the finite-sample stability, bias, and standard errors of the fitted models, as well as the robustness of the models' parameters. The same framework is applied to the proposed and competing models as well, to maintain consistency in the basis for the comparison of models.

4.1. Application to Survival Dataset

The empirical analysis was conducted using the Myeloma survival dataset [23], containing 65 observations and seven variables, in which x_1 refers to the logarithm of blood urea nitrogen (BUN), x_2 is hemoglobin, x_3 is the age, x_4 is the sex, and x_5 is the serum calcium. These are used as predictor variables. The variable time represents the observed survival time, while δ indicates whether the event occurred, with 1 denoting an observed event and 0 denoting a censored observation. The five covariates consist of three continuous variables x_1, x_2, and x_5 with x_3 being recorded as an integer-valued measurement and the binary variable x_4. The dataset contains 35 observed events and 30 censored observations, corresponding to an event rate of 53.85% and a censoring proportion of 46.15%. The survival time ranges from 1 to 92 units, with a mean of 24.0200 and a standard deviation of 23.7100. The median survival time is 15 units, indicating a right-skewed distribution, with the upper quartile reaching 35 units. For the covariates, x_1 has a mean of 1.3920 and ranges from 0.7780 to 2.2360, while x_2 has a mean of 10.2020 and ranges from 4.9000 to 14.6000. Variable x_3 has a mean of 60.154, with values ranging from 38 to 82. The binary variable x_4 has a mean of 0.4150, indicating that approximately 41.5% of observations have a value of 1. Variable x_5 has a mean of 10.1230 and ranges from 7 to 18. Table 5 summarizes the descriptive characteristics of the variables used in the analysis.

Table 5. Descriptive statistics of the Myeloma dataset.

Variable	Mean	SD	Min	25%	Median	75%	Max
time	24.0150	23.7130	1.0000	7.0000	15.0000	35.0000	92.0000
δ	0.5380	0.5020	0.0000	0.0000	1.0000	1.0000	1.0000
x_1	1.3920	0.3120	0.7780	1.1460	1.3220	1.5680	2.2360
x_2	10.2020	2.5580	4.9000	8.8000	10.2000	12.0000	14.6000
x_3	60.1540	10.3340	38.0000	51.0000	60.0000	67.0000	82.0000
x_4	0.4150	0.4970	0.0000	0.0000	0.0000	1.0000	1.0000
x_5	10.1230	1.8160	7.0000	9.0000	10.0000	10.0000	18.0000

4.2. Maximum Likelihood Estimation

Suppose that $\mathcal{D} = \{(t_i, \delta_i) : i = 1, \ldots, n\}$ denotes a right-censored survival dataset, where $t_i > 0$ is the observed time for the ith individual and δ_i is the censoring indicator. Specifically, $\delta_i = 1$ if the failure time is observed and $\delta_i = 0$ if the failure time is right-censored. The observed time is given by $t_i = \min(T_i, C_i)$, where T_i denotes the failure time and C_i denotes the censoring time.

$$\delta_i = \begin{cases} 1, & \text{if the event is observed,} \\ 0, & \text{if the observation is right censored.} \end{cases} \tag{58}$$

Alternatively, $t_i = \min(X_i, C_i), \delta_i = I(X_i \leq C_i)$, where C_i is the censoring time and X_i is the latent failure time. The observed data are the pairs (t_i, δ_i) for $i = 1, \ldots, n$, assuming the censoring mechanism is non-informative.

Define the parameter vector of the proposed WGECR model as $\boldsymbol{\eta} = (\alpha, \beta, \lambda, \theta)^\top$, where $\alpha, \beta, \lambda, \theta > 0$. The numbers of failures and censored observations are, respectively, $n_f = \sum_{i=1}^{n} \delta_i$, $n_c = \sum_{i=1}^{n} (1 - \delta_i)$, and $\widehat{p}_c = \frac{n_c}{n}$. When the observations are right-censored, the likelihood function is given by

$$L(\boldsymbol{\eta}) = \prod_{i=1}^{n} [f(t_i; \boldsymbol{\eta})]^{\delta_i} [S(t_i; \boldsymbol{\eta})]^{1-\delta_i}, \tag{59}$$

where $S(t_i; \boldsymbol{\eta})$ and $f(t_i; \boldsymbol{\eta})$ are the survival function and PDF of the WGECR model given in (6) and (9), respectively. Substituting these models into (59), we get

$$\begin{aligned} L(\boldsymbol{\eta}) = \prod_{i=1}^{n} \Bigg\{ & \exp(-\beta t_i^\theta) \Big[\beta\theta t_i^{\theta-1} \{1 - (1 - \exp(-\lambda t_i))^\alpha\} + \alpha\lambda \exp(-\lambda t_i) \\ & (1 - \exp(-\lambda t_i))^{\alpha-1} \Big] \Bigg\}^{\delta_i} \times \Big\{ \exp(-\beta t_i^\theta) \big[1 - (1 - \exp(-\lambda t_i))^\alpha\big] \Big\}^{1-\delta_i} \\ = & \prod_{i=1}^{n} \Big[\exp(-\beta t_i^\theta) D_i \Big]^{\delta_i} \Big[\exp(-\beta t_i^\theta) A_i \Big]^{1-\delta_i}, \end{aligned} \tag{60}$$

where $C_i = 1 - \exp(-\lambda t_i)$, $A_i = 1 - C_i^\alpha = 1 - (1 - \exp(-\lambda t_i))^\alpha$, and $D_i = \beta\theta t_i^{\theta-1} A_i + \alpha\lambda \exp(-\lambda t_i) C_i^{\alpha-1}$.

The log-likelihood function of (60) is

$$\ell(\boldsymbol{\eta}) = \sum_{i=1}^{n} \delta_i \Big[-\beta t_i^\theta + \log(D_i) \Big] + \sum_{i=1}^{n} (1 - \delta_i) \Big[-\beta t_i^\theta + \log(A_i) \Big]. \tag{61}$$

The MLE of the parameter vector is $\widehat{\boldsymbol{\eta}} = \underset{\boldsymbol{\eta} \in \Theta}{\arg\max}\ \ell(\boldsymbol{\eta})$, with the parameter space $\Theta = \{(\alpha, \beta, \lambda, \theta) : \alpha, \beta, \lambda, \theta > 0\}$.

The partial derivative with respect to α is

$$\frac{\partial \ell}{\partial \alpha} = \sum_{i=1}^{n} \delta_i \frac{-\beta\theta t_i^{\theta-1} C_i^\alpha \log(C_i) + \lambda \exp(-\lambda t_i) C_i^{\alpha-1} [1 + \alpha \log(C_i)]}{D_i} - \sum_{i=1}^{n} (1 - \delta_i) \frac{C_i^\alpha \log(C_i)}{A_i}. \tag{62}$$

The partial derivative with respect to β is

$$\frac{\partial \ell}{\partial \beta} = \sum_{i=1}^{n} \delta_i \left[-t_i^\theta + \frac{\theta t_i^{\theta-1} A_i}{D_i} \right] - \sum_{i=1}^{n} (1 - \delta_i) t_i^\theta. \tag{63}$$

The partial derivative with respect to λ is

$$\frac{\partial \ell}{\partial \lambda} = \sum_{i=1}^{n} \delta_i \frac{-\alpha\beta\theta t_i^{\theta} \exp(-\lambda t_i) C_i^{\alpha-1} + \alpha \exp(-\lambda t_i) C_i^{\alpha-1}}{D_i} + \sum_{i=1}^{n} \delta_i \frac{-\alpha\lambda t_i \exp(-\lambda t_i) C_i^{\alpha-1} + \alpha(\alpha-1)\lambda t_i \exp(-2\lambda t_i) C_i^{\alpha-2}}{D_i} - \sum_{i=1}^{n} (1-\delta_i) \frac{\alpha t_i \exp(-\lambda t_i) C_i^{\alpha-1}}{A_i}. \quad (64)$$

Finally, the partial derivative with respect to θ is

$$\frac{\partial \ell}{\partial \theta} = \sum_{i=1}^{n} \delta_i \left[-\beta t_i^{\theta} \log(t_i) + \frac{\beta t_i^{\theta-1} A_i (1 + \theta \log(t_i))}{D_i} \right] - \sum_{i=1}^{n} (1-\delta_i) \beta t_i^{\theta} \log(t_i). \quad (65)$$

The likelihood equations do not have closed-form solutions, so numerical optimization is necessary to find the MLEs. The score vector is equal to $\boldsymbol{U}(\boldsymbol{\eta}) = \big(U_\alpha(\boldsymbol{\eta}), U_\beta(\boldsymbol{\eta}), U_\lambda(\boldsymbol{\eta}), U_\theta(\boldsymbol{\eta})\big)^\top$, where $U_\alpha(\boldsymbol{\eta}) = \frac{\partial \ell(\boldsymbol{\eta})}{\partial \alpha}$, $U_\beta(\boldsymbol{\eta}) = \frac{\partial \ell(\boldsymbol{\eta})}{\partial \beta}$, $U_\lambda(\boldsymbol{\eta}) = \frac{\partial \ell(\boldsymbol{\eta})}{\partial \lambda}$, $U_\theta(\boldsymbol{\eta}) = \frac{\partial \ell(\boldsymbol{\eta})}{\partial \theta}$. Therefore, the maximum likelihood estimates satisfy the nonlinear system $\boldsymbol{U}(\widehat{\boldsymbol{\eta}}) = \mathbf{0}$, that is, $U_\alpha(\widehat{\boldsymbol{\eta}}) = 0, U_\beta(\widehat{\boldsymbol{\eta}}) = 0$, $U_\lambda(\widehat{\boldsymbol{\eta}}) = 0, U_\theta(\widehat{\boldsymbol{\eta}}) = 0$. The parameters in the numerical implementation are restricted to the positive parameter space, $\alpha > 0, \beta > 0, \lambda > 0, \theta > 0$.

Due to the dependency of the sensitivity on the initial parameters, a few values of initial parameters are tested in the optimization process to minimize the sensitivity. The solutions obtained are evaluated for their convergence, parameter validity, and finiteness of the log-likelihood. Any solutions that correspond to invalid values of the parameters or to non-finite log-likelihood are neglected. The vector of parameters that maximizes the finite log-likelihood among the converged and admissible solutions is taken as the final maximum likelihood estimate. The package 'survival' is also made available for the computational implementation of the procedures of survival analysis.

4.3. Model Selection Criteria

The performance of the proposed WGECR model is compared to some of the other possible lifetime models. The following fitted competitors are considered: GE, Weibull (W), additive Weibull (AW) by [24], exponentiated generalized Weibull–Gompertz (EGWG) by [25], dual-failure competing risk (DFCR) by [26], exponentiated modified Weibull extension (EMWE) by [27], and Marshall–Olkin Weibull (MW) by [28]. The same right-censored likelihood in (59) is used for each distribution of candidates. Therefore, variations in model performance are not due to the methods used to treat censored observations but due to differences in the distributional assumptions. We use the maximized log-likelihood (LogL), Akaike information criterion (AIC), corrected Akaike information criterion (AICc), and Bayesian information criterion (BIC) to compare the fitted models. These are the criteria to be used to assess the compromise between goodness of fit and model complexity.

Define the maximized log-likelihood as $\widehat{\ell}$, the number of free estimated parameters as k and the number of all observations as n. The AIC is defined by the following equation:

$$\mathrm{AIC} = -2\ell(\widehat{\boldsymbol{\psi}}) + 2k. \quad (66)$$

The AIC is a measure of the relative quality of a fitted model which tries to balance the goodness of fit with the number of estimated parameters. The finite-sample correction of AIC is the AICc defined as

$$\text{AICc} = \text{AIC} + \frac{2k(k+1)}{n-k-1}, \qquad n > k+1, \tag{67}$$

where $n > k+1$. This correction is very important when the number of parameters of the model is larger than the sample size.

The BIC is defined as

$$\text{BIC} = -2\ell(\widehat{\boldsymbol{\psi}}) + k\log n. \tag{68}$$

A larger maximized LogL means the model fits the data well in terms of likelihood; smaller AIC, AICc, and BIC values mean the model fits well in terms of likelihood and is not too complex. These criteria are then compared to the other competing distributions that were fitted to the same dataset, under the same treatment of the right-censored observations. These information criteria can be used for comparison and should be used in conjunction with the goodness-of-fit and residual analyses.

Suppose that $\widehat{\boldsymbol{\psi}}$ is the maximum likelihood estimate. Under standard regularity conditions, its asymptotic covariance matrix is obtained from the inverse of the observed information matrix,

$$\widehat{\text{Var}}(\widehat{\boldsymbol{\psi}}) = \mathcal{I}(\widehat{\boldsymbol{\psi}})^{-1}, \tag{69}$$

where $\mathcal{I}(\widehat{\boldsymbol{\psi}}) = -\frac{\partial^2 \ell(\boldsymbol{\psi})}{\partial \boldsymbol{\psi} \partial \boldsymbol{\psi}^\top}\Big|_{\boldsymbol{\psi}=\widehat{\boldsymbol{\psi}}}$. Therefore, the standard error of the jth parameter is

$$\text{SE}(\widehat{\psi}_j) = \sqrt{\left[\widehat{\text{Var}}(\widehat{\boldsymbol{\psi}})\right]_{jj}}. \tag{70}$$

4.4. Cox–Snell Residuals Analysis

The adequacy of the models is also explained by the Cox–Snell residuals [29]. The fitted Cox–Snell residual is defined as follows for the ith observation.

$$r_i = -\log\left[\widehat{S}(t_i)\right]. \tag{71}$$

Under the correctly specified fitted model, Cox–Snell residuals will be approximately exponentially distributed with survival function $S_R(r) = \exp(-r)$.

Consider the Kaplan–Meier estimate of the residual survival function of interest $\widehat{S}_{R,\text{KM}}(r)$. The Cox–Snell discrepancy that was utilized for analysis is

$$D_{\text{CS}} = \sup_{r>0}\left|\widehat{S}_{R,\text{KM}}(r) - \exp(-r)\right|. \tag{72}$$

The closer the value of D_{CS} to zero, the more similar the empirical residual survival function to the theoretical standard exponential survival function.

The fitted survival functions are also compared with the nonparametric Kaplan–Meier estimator, in addition to numerical criteria. Let $\widehat{S}_j(t)$ denote the fitted survival function for model j. The graphical evaluation is based on comparing $\widehat{S}_j(t)$ to $\widehat{S}_{\text{KM}}(t)$. This comparison offers a graphical evaluation of the model's performance in capturing the observed survival curve over the set of observed follow-up times.

The goodness of fit of the proposed WGECR model is examined by comparing the model with some competing survival models using the LogL, AIC, AICc, BIC, and Cox–Snell discrepancy. The results are presented in Table 6. From the results presented, the proposed WGECR is the best-fitting model among the models tested. WGECR has the

largest LogL value (−166.9194) and the minimum AIC (341.8388), AICc (342.5055), and BIC (350.5363) values are the lowest of all the models considered for WGECR. The results show that WGECR yields a better trade-off between goodness of fit and model complexity in terms of all three information criteria. It is concluded that the results have come out as an optimum between the accuracy of the model and the complexity of the model.

Table 6. Likelihood-based model selection criteria and Cox–Snell goodness-of-fit measures for the fitted survival models.

Model	LogL	AIC	AICc	BIC	D_{CS}
WGECR	−166.9194	341.8388	342.5055	350.5363	0.2376
EMWE	−172.2723	352.5447	353.2113	361.2422	0.2757
EGWG	−172.0095	354.0191	355.0360	364.8910	0.3160
DFCR	−179.2442	366.4884	367.1551	375.1860	0.3928
AW	−184.9290	377.8580	378.5247	386.5556	0.2793
MW	−275.0330	556.0659	556.4594	562.5891	0.7974
W	−284.7121	573.4242	573.6177	577.7730	0.6307
GE	−289.3962	582.7923	582.9859	587.1411	0.7672

There is further evidence to support this comparison in the Cox–Snell diagnostic. The WGECR model has the least reported Cox–Snell discrepancy of $D_{CS} = 0.2376$, which means that the empirical residual survival function is closer to the theoretical standard exponential survival function than the other models. There are discrepancies of 0.2793 for the AW model and 0.2757 for the EMWE, but both are larger than that of WGECR. The rest of the models are also relatively large, with the MW model giving a value of 0.7974.

The proposed WGECR model is consistently the best choice in comparison to the other models that were considered, using the likelihood and Cox–Snell diagnostic criteria together. We present numerical evidence for this agreement that is complementary to the visual evidence presented above and confirms that the proposed distribution is a good fit to the observed survival data, but does not overcomplicate the analysis. However, these results do not prove that the WGECR model is always better than the other models in the set considered, but only that it is better than the remaining models in the set.

The Kaplan–Meier estimate of the survival function is given, along with the fitted survival functions of the proposed WGECR model and the competing models in Figure 3, to complement the comparison of the numerical models. The Kaplan–Meier is a nonparametric reference that can be used to check the fit of each fitted distribution in comparison to the survival pattern observed in the data. When the fitted survival curve is closer to the Kaplan–Meier estimate, the curve has a more realistic shape of the actual survival experience during the follow-up period.

The proposed WGECR model has relatively good agreement with the Kaplan–Meier curve as shown in the survival curve plot in Figure 3, whereas some of its competitors have larger differences. The overall survival pattern is checked using visual agreement to ensure good capture of the pattern by WGECR. The graphical comparison is in line with the numerical results presented in Table 6, which show that the WGECR model has the lowest AIC, AICc, BIC, and Cox–Snell discrepancy among the models considered. In addition, the close association with the Kaplan–Meier estimate gives support to the findings of the information-criterion analysis, since it gives a visual indication of the shape of the fitted survival function and the Cox–Snell diagnostic provides a visual assessment of the agreement between the empirical residual survival function and its theoretical counterpart.

Therefore, both the graphical and the numerical evidence support the best model selected from the list of models considered for this dataset being WGECR. The agreement of the visual plots is necessarily qualitative, but it is consistent with the likelihood-based criteria and residual diagnostics and adds to the overall feeling of model adequacy.

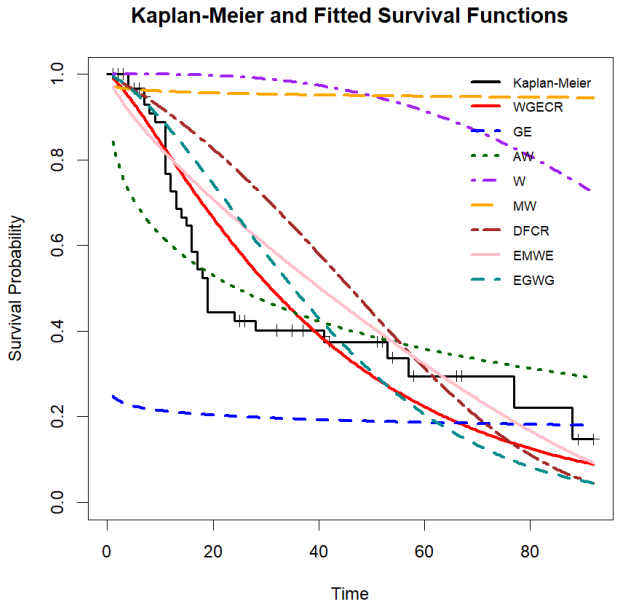


Figure 3. Kaplan–Meier estimate and fitted survival functions for the WGECR model and competing models.

The graphical comparison of Figure 3 is consistent with the numerical goodness-of-fit results in Table 6. Specifically, the relatively close agreement between the fitted WGECR survival function and the Kaplan–Meier estimate is confirmed by the WGECR survival function having the smallest AIC, AICc, BIC and Cox–Snell discrepancy values. Therefore, the following results of the graphical assessment, together with the competing models considered, give complementary evidence in favor of WGECR.

The Cox–Snell residual survival function estimates are also compared to the standard exponential survival function $S_R(r) = \exp(-r)$ to further investigate the model fit. This diagnostic comparison is shown in Figure 4. The WGECR residual curve is in relatively good agreement with the theoretical curve, with some of the competing models showing greater deviations. This is based on the graphical result of the Cox–Snell discrepancy value D_{CS}, which has the value of 0.2376, confirming that the proposed model is adequate.

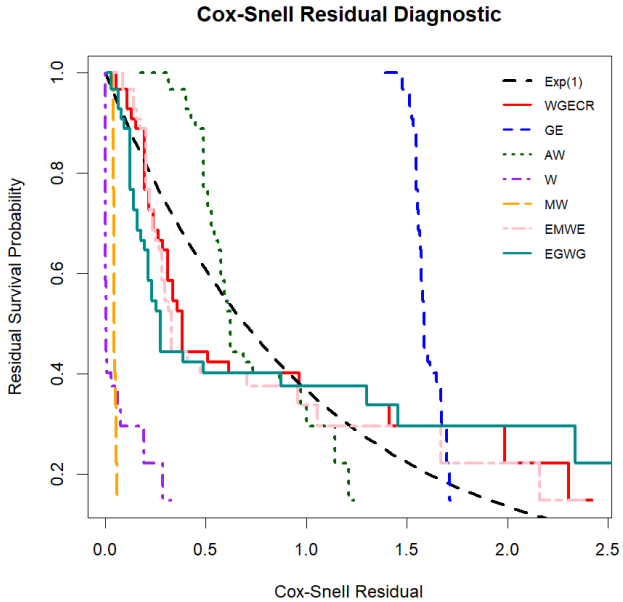


Figure 4. Cox–Snell residual survival functions for the WGECR model and competing models compared with the theoretical Exp(1) survival function.

4.5. Bootstrap Validation and Stability Analysis

The finite-sample stability of the proposed WGECR model is evaluated by a fully parametric bootstrap similar to the one used in [30].

Let $\widehat{\eta} = (\widehat{\alpha}, \widehat{\beta}, \widehat{\lambda}, \widehat{\theta})^\top$ be the WGECR MLE. The number of bootstrap replications is $B = 2000$. Event times are generated from $F(t; \widehat{\boldsymbol{\eta}})$ for the bth bootstrap replication ($b = 1, \ldots, B$).

Let $U_i^{*(b)} \sim U(0,1)$. The failure time generated is given by

$$F(X_i^{*(b)}; \widehat{\boldsymbol{\eta}}) = U_i^{*(b)}, \tag{73}$$

or equivalently,

$$X_i^{*(b)} = F^{-1}\left(U_i^{*(b)}; \widehat{\boldsymbol{\eta}}\right). \tag{74}$$

The inverse distribution function is not analytically invertible, and thus the inverse equation is solved numerically via a one-dimensional root-finding algorithm.

To simulate the right-censoring mechanism, the censoring times $C_i^{*(b)}$ are simulated from a fitted Weibull distribution, Weibull(β_c, θ_c), where the estimated censoring parameters are obtained from the observed censored times. The observed time with bootstrapping is

$$T_i^{*(b)} = \min\left\{X_i^{*(b)}, C_i^{*(b)}\right\}, \tag{75}$$

with event indicator

$$\delta_i^{*(b)} = I\left(X_i^{*(b)} \leq C_i^{*(b)}\right). \tag{76}$$

Therefore, the basic structure of each bootstrap dataset is the same as the original right-censored survival data.

For every valid replication, the WGECR model is refitted with the parameter vector $\widehat{\boldsymbol{\eta}}^{*(b)} = \left(\widehat{\alpha}^{*(b)}, \widehat{\beta}^{*(b)}, \widehat{\lambda}^{*(b)}, \widehat{\theta}^{*(b)}\right)^\top$ being stored. The validity of a bootstrap replication depends on the success of a fit of the generated data, convergence of the numerical optimization, the existence of a finite maximized log-likelihood, and the existence of finite parameter estimates from the WGECR.

$$\widehat{\beta}^* > 0, \qquad \widehat{\theta}^* > 0, \qquad \widehat{\lambda}^* > 0, \qquad \widehat{\alpha}^* > 0.$$

The number of requested and valid bootstrap replications is being recorded to assess the numerical stability of the estimation procedure. Define B_v to be the number of valid replications of the bootstrap. Selected threshold exceedance probabilities and the upper tail quantiles of the empirical bootstrap distribution of the parameter α of the WGECR are also analyzed. The exceedance probability for a given threshold $c > 0$ is given by the bootstrap exceedance probability

$$\widehat{P}_\alpha(c) = \frac{1}{B_v} \sum_{b=1}^{B_v} I\left(\widehat{\alpha}^{*(b)} > c\right). \tag{77}$$

This additional analysis is used to identify possible numerical and/or inferential instabilities of the estimated shape parameter.

The bootstrapped mean of parameter η_j is

$$\overline{\eta}_j^* = \frac{1}{B_v} \sum_{b=1}^{B_v} \widehat{\eta}_j^{*(b)}, \tag{78}$$

where B_v is the number of valid bootstrap replications. The bias from the bootstrap is

$$\widehat{\text{Bias}}(\widehat{\eta}_j) = \overline{\eta}_j^* - \widehat{\eta}_j, \tag{79}$$

and the standard error of the bootstrap is

$$\widehat{\mathrm{SE}}_B(\widehat{\eta}_j) = \left[\frac{1}{B_v - 1}\sum_{b=1}^{B_v}\left(\widehat{\eta}_j^{*(b)} - \overline{\eta}_j^{*}\right)^2\right]^{1/2}. \tag{80}$$

The 95% bootstrap confidence interval is

$$\mathrm{CI}^{*}_{j,0.95} = \left[\widehat{\eta}^{*}_{j,0.025}, \widehat{\eta}^{*}_{j,0.975}\right]. \tag{81}$$

The log-likelihood and the main information criteria are maximized for each valid bootstrap replication and used to assess the stability of model selection. As a result, the bootstrap method gives repeated-sample evidence of the relative performance of the proposed WGECR model and the competing distributions.

The bootstrap procedure is also used to assess the stability of the Cox–Snell goodness-of-fit statistic. Define the Cox–Snell statistic D_{obs} from the original WGECR fit and the statistic $D^{*(b)}_{\mathrm{obs}}$ from the bth bootstrap sample. Define D_{obs} as the Cox–Snell statistic based on the original WGECR fit and $D^{*(b)}_{\mathrm{obs}}$ as the Cox–Snell statistic based on the bth bootstrap sample. The probability is obtained by the following calculation using the bootstrap Monte Carlo method.

$$p_{\mathrm{boot}} = \frac{\left[1 + \sum_{b=1}^{B_v} I\left(D^{*(b)} \geq D_{\mathrm{obs}}\right)\right]}{B_v + 1}. \tag{82}$$

A Cox–Snell summary is defined as the mean, standard deviation, median, and the percentile limits for the bootstrap distribution.

The proportion of censored observations in each of the bootstrap samples is given by

$$\widehat{p}_c^{*(b)} = \frac{1}{n}\sum_{i=1}^{n} I\left(\delta_i^{*(b)} = 0\right). \tag{83}$$

The average value of the 100 bootstraps is

$$\overline{p}_c^{*} = \frac{1}{B_v}\sum_{b=1}^{B_v}\widehat{p}_c^{*(b)}. \tag{84}$$

The observed proportion of censored observations is compared with the bootstrap proportion of censored observations to ensure that the fitted censoring mechanism is able to generate the observed censoring structure.

The finite-sample performance and numerical stability of these estimates are then explored by means of the parametric bootstrap approach outlined in Section 4.5. This procedure involves 2000 replications to assess the variability of the parameter estimates, the bootstrap bias, the standard errors, percentile confidence intervals, and the stability of the fitted model. Each valid bootstrap sample is used to refit the same maximum likelihood estimation model.

The WGECR model is refitted for each bootstrap replication, using the maximum likelihood estimation procedure outlined in Section 4.2. Several starting values are allowed and if convergence occurs, the solution having the maximum finite log-likelihood value is kept in the set of the admissible solutions, which is considered to be not sensitive to the starting point. The replications with invalid parameter values or non-finite log-likelihood values are considered unsuccessful fits and are not included in the valid bootstrap replications. The means, biases, standard errors, and percentile confidence intervals of the retained estimates are used to compute the bootstrap means, biases, standard errors, and

percentile confidence intervals. Additionally, the results at convergence for each of the replications are analyzed to evaluate the numerical stability of the estimation procedure.

All calculations are done in R. The packages `maxLik` and `survival` are for maximum likelihood estimation and survival analysis procedures, respectively. The distribution function of the WGECR is numerically inverted with the `uniroot` algorithm.

To estimate the sampling variability of the parameter estimates and the reference distribution of the Cox–Snell goodness-of-fit statistic, we used $B = 2000$ parametric bootstrap replications. This is simply a practical balance between the precision of the Monte Carlo method and computation, since in each replication, the numerical parameter estimation is needed. The seed for random numbers was fixed to make the results reproducible. The Monte Carlo error could be reduced with more replications, but the number of replications used here, $B = 2000$, gives strong grounds for the bootstrap summaries in this study. Analysis results include estimates of the survival function parameters, their standard errors, Cox–Snell survival function statistics, fitted survival functions, validity statistics for the proposed model, validity statistics for the proposed model (bootstrap), bootstrap bias, bootstrap standard errors, percentile confidence intervals, and censoring summaries of the proposed model and the competing distributions.

Using a parametric bootstrap analysis, the sampling variability and uncertainty of the maximum likelihood estimates were estimated. Table 7 is provided to get further insight into the finite-sample properties of the maximum likelihood estimates, obtained by using the bootstrap. The biases of the bootstrap estimates of θ and λ are relatively small, namely 0.0468 and 0.0052, respectively, which indicates that the bootstrap is a reasonable approximation of the maximum likelihood estimates. The variability of the bootstrap distribution of α is significantly larger, in contrast. The bootstrap mean is 16.6941 and the maximum likelihood estimate is 1.3507, for a positive bias of 15.3434 and a standard error (SE) of 70.1158. There is also considerable uncertainty in the estimation of this parameter, as shown by the wide 95% confidence interval: 0.9451 to 244.4116.

Table 7. Bootstrap estimates, bias, standard errors, and 95% confidence intervals for the WGECR model parameters.

Parameter	MLE	Mean	Bias	SE	Lower 95%	Upper 95%
β	2.89×10^{-7}	0.0067	0.0067	0.0095	3.100×10^{-8}	0.0296
θ	1.0156	1.0626	0.0468	0.4290	0.42056	2.9164
λ	0.0295	0.0347	0.0052	0.0232	2.07×10^{-7}	0.0994
α	1.3507	16.6941	15.3434	70.1158	0.9451	244.4116

This is consistent with the highly right-skewed bootstrap distribution of α, with most estimates being on the low end of the distribution, and a relatively small number of large estimates pushing the upper tail. This seriously overestimates the bootstrap mean and standard error. The results indicate that estimating α could be sensitive to sampling variation and to the numerical properties of the likelihood function. Given the above, caution should be taken when interpreting its point estimate, especially when making inferences about the shape characteristics of the model. This discovery does not mean that the WGECR model is incorrect, but rather that there is an important limitation in the finite-sample precision of this parameter estimate.

The Cox–Snell discrepancy statistic was then used to assess the goodness of fit of the proposed model for the 2000 replications of a parametric bootstrapping method.

Table 8 shows a goodness-of-fit test for the Cox–Snell discrepancy statistic using a parametric bootstrap. The difference found for WGECR is $D_{CS} = 0.2376$, and the p-value is determined from 2000 replications and is equal to 0.0720. This p-value is greater than

the preset level of significance (5%); thus, this test is not sufficient to reject the fitting of the WGECR model at 5%. The results under the bootstrap procedure therefore do not indicate, and will not indicate, that the model is an inadequate fit to the data.

Table 8. Parametric bootstrap goodness-of-fit assessment for the WGECR model.

Model	D_{CS}	Bootstrap p-Value	B	Valid B	Successful Fits
WGECR	0.2376	0.0720	2000	2000	2000

The distribution of the goodness-of-fit test for Cox–Snell is shown in Figure 5 along with the observed value of the test. The observed value $D_{CS} = 0.2376$ is in the upper tail of the bootstrap distribution, but is still in the 95% bootstrap interval (0.0707, 0.2892). This value is consistent with the result of the bootstrap test and is close to the center of the range that corresponds to the interval reported. Furthermore, the validity and success of the model fits were obtained in all 2000 replications of the bootstrapping procedure, which implies that the procedure was completed successfully throughout the analysis.

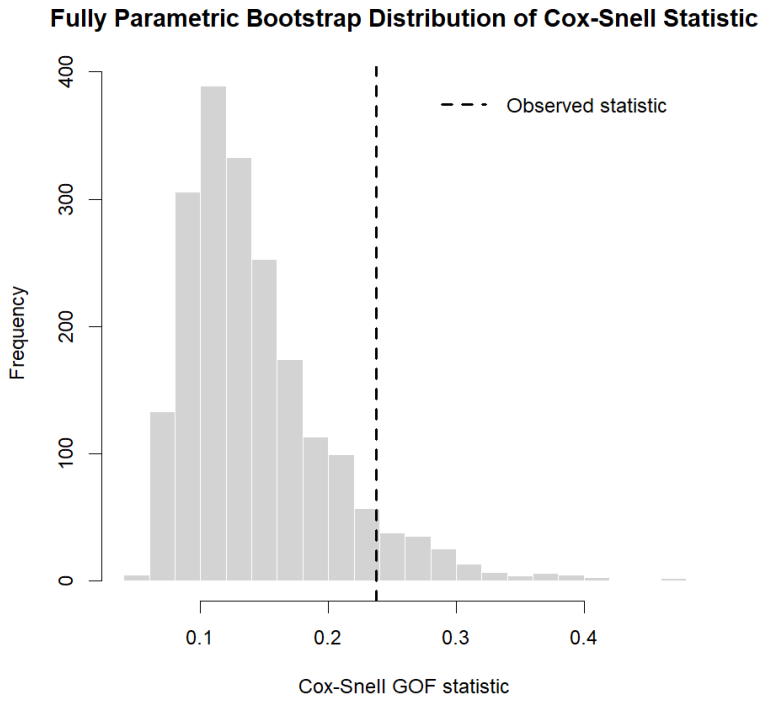


Figure 5. Parametric bootstrap distribution of the Cox–Snell goodness-of-fit statistic for the WGECR model. The dashed vertical line indicates the observed statistic, $D_{CS} = 0.2376$.

The results as a whole are supportive but not conclusive evidence of the suitability of WGECR for the sample examined. However, a p-value of 0.0720 is not to be taken as a sign of the model being accurate or a 92.8% chance it is accurate. Instead, it suggests that the bootstrap goodness-of-fit test fails to reject the fitted model at the 5% significance level. This conclusion should be read in conjunction with the information criteria, the comparison of the survival functions, and other diagnostic results provided previously in the manuscript.

In order to further explore the bootstrap stability of the estimates of the WGECR parameters, the distribution of the parameter α is plotted in Figure 6 for this parameter on a logarithmic scale. The distribution of the bootstrap values of α is highly right skewed, with a long tail at the upper end of the range. Most of the values of the bootstrap are near the low end of the range. This suggests that the large variability of the bootstrap values of α is predominantly due to a relatively small number of extreme values.

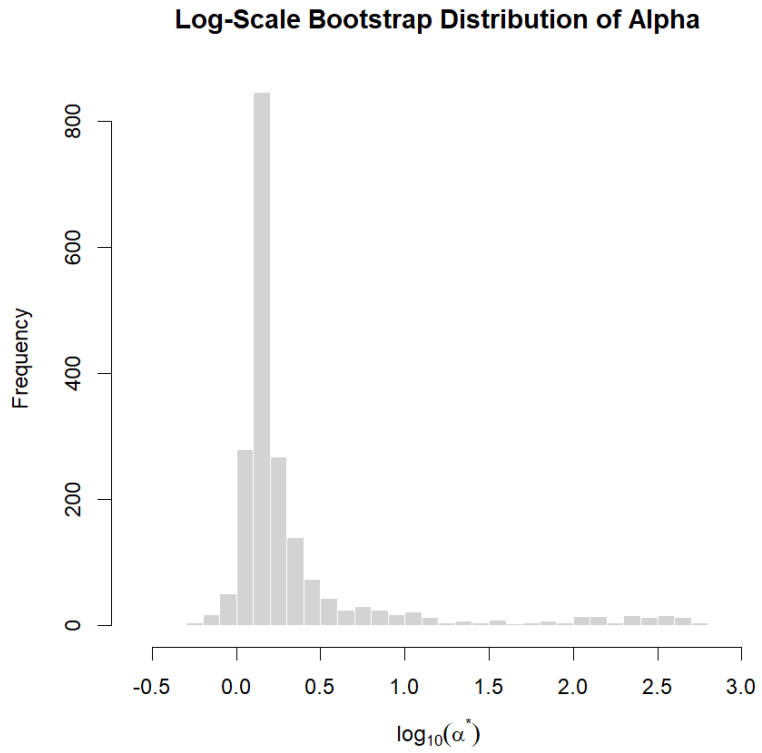


Figure 6. Log-scale parametric bootstrap distribution of the WGECR parameter α.

The results of the bootstrap were then analyzed separately based on the central region ($\alpha \leq 100$), and the extreme region ($\alpha > 100$) to check the stability of the estimates of the bootstrap parameters. The cases are summarized in Tables 9 and 10 for $\alpha \leq 100$, and $\alpha > 100$, respectively.

Table 9. Bootstrap summary statistics for parameter estimates with $\alpha \leq 100$.

Parameter	Minimum	Q1	Median	Mean	Q3	Maximum
β	0.0000	2.52×10^{-7}	4.30×10^{-7}	0.0062	0.0125	0.0471
θ	2.8×10^{-4}	0.9490	1.0233	1.0609	1.0863	3.8882
λ	1.00×10^{-8}	0.0234	0.0333	0.0313	0.0407	0.1351
α	0.2863	1.3448	1.4999	3.0202	1.9123	82.7361

Table 10. Bootstrap summary statistics for parameter estimates with $\alpha > 100$.

Parameter	Minimum	Q1	Median	Mean	Q3	Maximum
β	0.0030	0.0101	0.0145	0.0160	0.0190	0.0454
θ	0.7446	0.9771	1.0830	1.0950	1.1829	1.6204
λ	0.0471	0.0791	0.0989	0.0995	0.1141	0.2261
α	101.9000	149.6000	250.0000	282.1000	366.4000	978.3000

The summary of the bootstrapped estimates of the parameters in the central region ($\alpha \leq 100$) and in the extreme region ($\alpha > 100$) is displayed in Tables 9 and 10, respectively. The median values of the parameters θ, λ, α are respectively 1.0233, 0.0333 and 1.4999 for $\alpha \leq 100$ and provide a good intuition of a reasonable concentration of the bootstrap estimates. The latter, the $\alpha > 100$ region, has a very different extreme tail, having a median α of 250.0000, a mean of 282.1000 and a maximum of 978.3000. The parameters look fairly stable in the middle of the distribution, but there are some very high values on the tail of the distribution (high values of α) that appear to have large variations.

5. Distribution-Informed Survival Feature Transformation Using WGECR for Random Survival Forest Prediction

Survival analysis is concerned with modeling the time until the occurrence of an event while appropriately accounting for right censoring and other incomplete observations. It is widely applied in medical prognosis, reliability, finance, engineering, and risk management, where the objective extends beyond predicting whether an event will occur to estimating the probability of surviving beyond a specified time. Traditional approaches, particularly the Cox proportional hazards model and parametric survival distributions, provide interpretable statistical methods but may impose restrictive assumptions regarding covariate effects and the underlying hazard structure. Recent developments in machine learning (ML) have therefore provided important alternatives for capturing nonlinear and complex relationships in time-to-event data [31–33]. Systematic reviews indicate a rapid expansion of ML and deep-learning methods for survival prediction, although methodological challenges remain concerning model specification, censoring, interpretability, feature representation, and reliable evaluation [34].

Among ML survival methods, Random Survival Forest (RSF) has attracted considerable attention because it extends the random forest principle to right-censored data without requiring the proportional-hazards assumption. The original RSF formulation of [32] introduced survival-specific splitting rules and ensemble-based estimation of mortality and survival functions. More recent studies continue to demonstrate the usefulness of RSF for nonlinear risk prediction and patient stratification. For example, [35] used RSF to investigate the combined effects of multiple physiological risk factors on mortality, while recent methodological work has extended RSF to functional and more complex survival data structures [36]. Garcia-Lopez et al. [37] further demonstrated the practical application of RSF in time-to-event prediction and emphasized the importance of appropriate training, cross-validation, and evaluation procedures. These developments confirm the continuing relevance of RSF as a flexible survival-learning algorithm. Nevertheless, conventional RSF generally receives the observed covariates directly and relies on recursive partitioning to discover useful nonlinear relationships. Consequently, the quality of the representation supplied to the learner remains an important but relatively underexplored component of survival prediction.

An alternative perspective is to exploit the statistical information contained in probability distributions before applying ML algorithms. Flexible probability distributions have long been developed to accommodate skewness, heavy tails, multimodality, and non-monotonic hazard structures that may not be adequately represented by conventional survival distributions. Recent work continues this direction by constructing extended distribution families capable of representing a wider range of failure-time behaviors. For example, [38] proposed an exponentiated-Weibull proportional-hazards model capable of accommodating both monotonic and non-monotonic baseline hazard shapes. Similarly, [39] developed a new Marshall–Olkin Lomax distribution with applications to failure and insurance data, illustrating the continuing importance of flexible Lomax-type distributions for heterogeneous lifetime and risk data. Such developments demonstrate that probability distributions can provide structured representations of complex data rather than serving only as standalone parametric models.

Recent research has also begun to connect newly developed probability distributions directly with ML prediction. Particularly relevant is the work of [40], who introduced a new Log-Lomax distribution and subsequently derived distribution-based features for ML prediction. Their study compared models using raw observations with models incorporating features derived from the Log-Lomax distribution and reported improved predictive performance for Random Forest and XGBoost across stock-exchange and heart-attack datasets.

This provides an important methodological indication: Information extracted from a fitted probability distribution can serve as a useful feature representation for an ML model. However, the Log-Lomax study primarily considered prediction using distribution-derived features in a general ML setting, leaving open the question of whether a survival function from a flexible distribution can be systematically used as a survival-oriented representation for a dedicated time-to-event learner such as RSF.

Despite these advances, an important gap remains in survival modeling. Existing ML survival studies have largely concentrated on modifying the learner, developing new neural architectures, improving tree-based survival algorithms, or combining multiple prediction models [34,36,37]. Conversely, research on flexible probability distributions has predominantly focused on parameter estimation, goodness of fit, hazard-shape flexibility, and standalone survival or reliability applications [38,39]. Although recent work such as the Log-Lomax-ML study [40] demonstrates the potential of distribution-derived features, there is limited research investigating whether the survival function itself can be used as a statistically informed feature representation for a conventional survival-learning algorithm. This distinction is important because the survival function provides a direct probabilistic interpretation: For a predetermined prediction horizon τ, $S(\tau \mid X_j)$ represents the model-based probability of surviving beyond τ conditional on predictor X_j. Such a representation can potentially convert heterogeneous raw measurements into a common survival-probability scale while retaining nonlinear information induced by the underlying distribution.

The present study addresses the identified gap by proposing a Hybrid RSF that integrates the original covariates with survival-probability features derived from the WGECR distribution. Each predictor is first modeled using the covariate-dependent WGECR distribution, and its estimated survival function is evaluated at a predetermined prediction horizon to obtain the corresponding survival-probability feature τ, $S_j(\tau \mid X_j)$. These distribution-informed features are then combined with the original covariates and supplied to the conventional RSF algorithm. Thus, the internal structure, splitting mechanism, and ensemble-learning procedure of RSF remain unchanged. To assess the contribution of the WGECR-based representation, three configurations are evaluated: Conventional RSF, which uses only the original covariates; WGECR-RSF, which uses only the WGECR-derived survival-probability features; and the proposed Hybrid RSF, which combines both original and WGECR-derived features. This comparative design enables the contribution of the WGECR transformation and the additional predictive value of retaining the original covariates to be systematically examined. The contribution of this paper is as follows:

i. A feature-transformation approach is proposed in which the WGECR distribution converts individual covariates into survival-probability features at a predetermined prediction horizon.
ii. The WGECR-derived survival-probability features are combined with the original covariates to form the input representation of the proposed Hybrid RSF, while the underlying RSF algorithm remains unchanged.
iii. Three configurations, Conventional RSF, WGECR-RSF, and Hybrid RSF, are systematically compared to determine the predictive contribution of the WGECR-derived features and the value of combining them with the original covariates.
iv. The study provides a general strategy for combining flexible distributional modeling with machine-learning survival analysis through feature representation, without requiring modification of the underlying learning algorithm.

5.1. Development of the WGECR-RSF Model

This section presents the proposed methodology for integrating the WGECR distribution with RSF through a survival-probability feature transformation. The central idea is to transform each original predictor into a distribution-informed survival-probability representation using the WGECR model before applying RSF. Unlike approaches that modify the internal structure or splitting mechanism of RSF, the proposed approach retains the conventional RSF algorithm and introduces the contribution of WGECR exclusively at the feature-representation level. This allows the predictive contribution of the distribution-based transformation to be evaluated independently of changes to the underlying ML algorithm. The methodology comprises data preprocessing, covariate-dependent WGECR estimation, survival-probability feature transformation, RSF modeling, prediction, and performance evaluation. The methodological diagram of the proposed Hybrid RSF is illustrated in Figure 7, while the overall procedure is summarized in Figure 8.

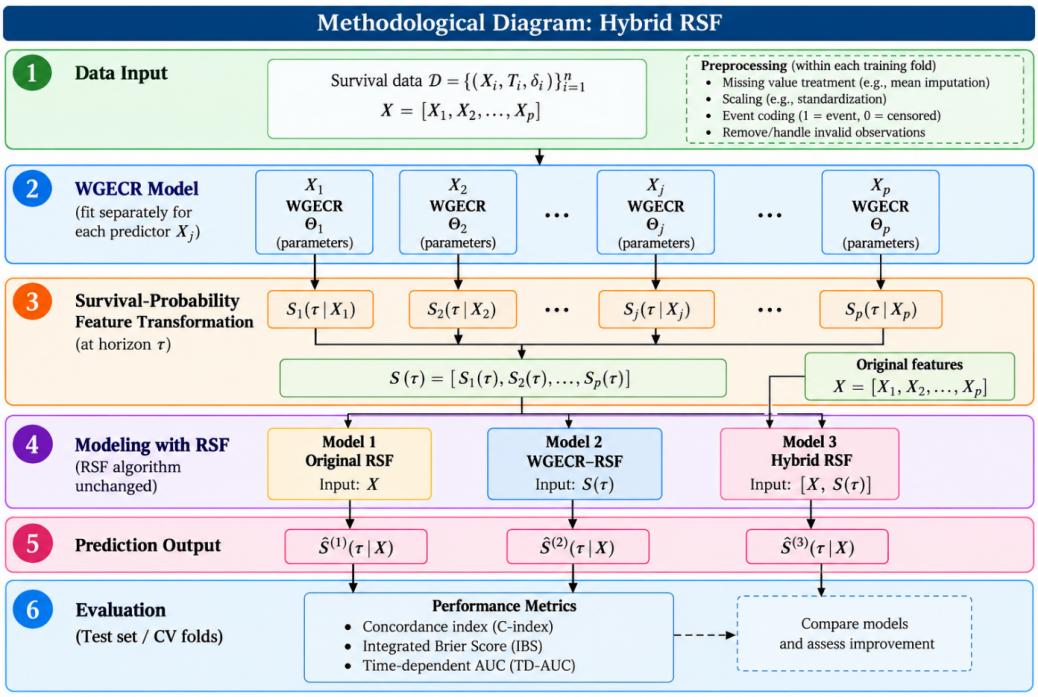


Figure 7. Methodological diagram of the proposed Hybrid RSF.

5.1.1. Methodological Framework

The proposed method integrates the WGECR probability model with RSF through a feature-level transformation. Each predictor X_j is first converted into a survival-probability feature $S_j(\tau \mid X_j)$, which is then supplied to the conventional RSF:

$$X_j \rightarrow WGECR \rightarrow S_j(\tau \mid X_j) \rightarrow RSF \rightarrow \hat{S}(t \mid X).$$

5.1.2. Data Preprocessing

Missing values are treated within the training data, continuous predictors are appropriately scaled, and event status is coded as 0 for censoring and 1 for the event. Invalid or non-finite observations are identified and handled before model fitting. To prevent information leakage, all preprocessing and distributional parameter estimation are performed using the training portion of each cross-validation fold and subsequently applied to the corresponding test fold.

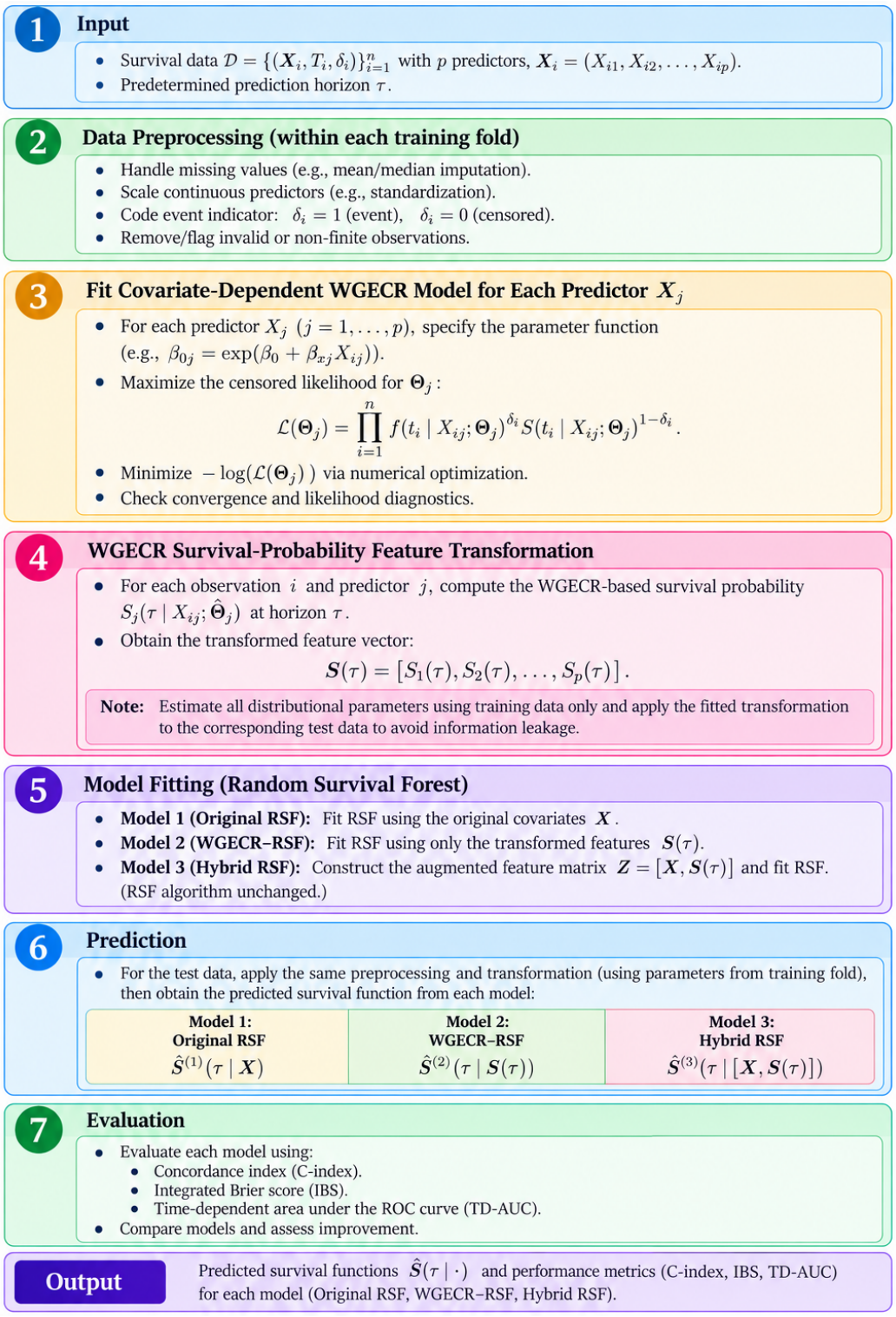


Figure 8. Algorithmic procedure for the proposed WGECR-informed Hybrid RSF.

5.1.3. Covariate-Dependent WGECR Model

For each predictor X_j, the WGECR parameters are allowed to depend on the observed covariate. For example, a positive parameter is defined as

$$\beta_{ij} = \exp(\beta_{0j} + \beta_{xj} X_{ij}), \tag{85}$$

ensuring parameter positivity. The corresponding survival probability at a predetermined horizon τ is then written as

$$S_{ij}(\tau) = S(\tau \mid X_{ij}; \Theta_j), \tag{86}$$

where Θ_j denotes the WGECR parameters associated with predictor X_j. This produces one distribution-derived survival feature for each predictor.

5.1.4. WGECR Survival-Probability Feature Transformation

The central transformation is

$$X_j \to S_j(\tau \mid X_j). \tag{87}$$

Consequently, the original predictor vector is transformed as

$$(X_1, \ldots, X_p) \to (S_1(\tau), \ldots, S_p(\tau)). \tag{88}$$

This transformation represents each predictor on a survival-oriented probability scale and incorporates distributional information that is not explicitly present in its original measurement scale. A predetermined prediction horizon τ is used rather than the patient's observed survival time, thereby avoiding target leakage.

5.1.5. Parameter Estimation

The WGECR parameters are estimated using the censored likelihood provided in (59). Parameter estimation is performed by minimizing the negative log-likelihood denoted as $-\log L(\Theta)$. Numerical optimization incorporates appropriate parameter constraints and initialization. Convergence and likelihood values are examined to ensure valid parameter estimates before generating the transformed features.

Random Survival Forest is used as the downstream survival-learning algorithm [32]. The forest receives the WGECR-derived features and estimates individual survival functions through its standard ensemble procedure. No modification is made to the internal splitting, tree-growing, or ensemble mechanism of RSF. The methodological intervention occurs exclusively at the feature-representation level.

5.1.6. WGECR-RSF

The WGECR-RSF model uses only the distribution-derived survival-probability features:

$$\mathbf{S}(\tau) \to RSF, \tag{89}$$

where $\mathbf{S}(\tau) = [S_1(\tau), S_2(\tau), \ldots, S_p(\tau)]$. Thus, the original predictors are replaced by their WGECR survival-probability representations before RSF estimation.

5.1.7. Proposed Hybrid RSF

The proposed Hybrid RSF integrates the original covariate representation with the survival-probability features generated from the WGECR model:

$$[\mathbf{X}, \mathbf{S}(\tau)] \to RSF. \tag{90}$$

This formulation determines whether the raw predictors provide additional predictive information beyond that already captured by the WGECR transformation.

5.1.8. Experimental Design

The experimental design compares three survival-learning configurations under the same data partitioning, cross-validation procedure, and evaluation criteria. The dataset

is divided into training and testing sets using an 80:20 split, while model robustness is assessed through repeated 5-fold cross-validation on the training data. The models are evaluated using the concordance index (C-index), integrated Brier score (IBS), and time-dependent AUC (TD-AUC).

Model 1—Original RSF: The conventional RSF is fitted directly using the original predictor variables and serves as the baseline.

Model 2—WGECR-RSF: The original predictors are transformed into WGECR survival-probability features at a predetermined horizon τ, which are then supplied to an otherwise standard RSF.

Model 3—Hybrid RSF: The Hybrid RSF uses both the original and WGECR-transformed features to determine whether the raw predictors provide additional information beyond the distribution-informed representation.

For each cross-validation fold, preprocessing and WGECR parameter estimation are performed using the training data only and subsequently applied to the corresponding test data to prevent information leakage. Model performance is summarized using the mean and standard deviation across repeated folds, supplemented by statistical significance testing and bootstrap confidence intervals. All analyses are implemented in Python using Google Colab, with the computational environment and required packages configured within the Colab runtime. Survival modeling, feature transformation, model fitting, and performance evaluation are performed using established Python libraries for survival analysis and ML.

5.2. Result and Discussion of the Hybrid RSF

The Myeloma dataset comprised 65 observations and five predictors $(x_1 - x_5)$. Of the 65 patients, 35 experienced the event, and 30 were censored, corresponding to an event proportion of 53.85%. Survival times ranged from 1 to 92 time units. These characteristics are summarized in Table 11.

Table 11. Characteristics of the Myeloma dataset.

Characteristic	Value
Sample size	65
Predictors	5
Events	35
Censored	30
Event proportion	53.85%
Minimum survival time	1
Maximum survival time	92

5.2.1. WGECR Parameter Estimates

The WGECR model was fitted separately to each predictor to obtain feature-specific parameter estimates. As shown in Table 12, the estimated parameters varied across predictors, indicating heterogeneous relationships between the predictors and the survival distribution. The covariate coefficient, denoted by β_x, was positive for $x_1 - x_4$ and negative for x_5. All estimated distributional parameters satisfy the model's positivity constraints, and all five WGECR fits achieved successful numerical convergence. Here, β_0 denotes the baseline coefficient, while β_x represents the covariate coefficient associated with the predictor x. Unlike the distributional parameters, β_x is a regression coefficient and therefore may take either positive or negative values. A positive β_x indicates a positive association between the predictor and the corresponding model component, whereas a negative β_x indicates an inverse association.

Table 12. Feature-specific WGECR parameter estimates.

Feature	β	θ	γ	λ	α	NLL
x_1	0.0020	1.2146	1.2283	0.0249	1.4128	165.8062
x_2	0.0003	1.6242	0.9812	0.0281	1.3413	166.9278
x_3	0.0003	1.5433	1.3075	0.0265	1.3209	166.5565
x_4	0.0003	2.0478	1.0828	0.0270	1.3480	166.7298
x_5	0.0003	−2.7070	1.2808	0.0253	1.3194	165.8664

The estimates indicate that the WGECR transformation captures feature-specific distributional behavior rather than applying a common transformation to all predictors.

The estimated WGECR models were used to generate survival-probability features for each predictor. As presented in Table 13, the mean transformed values were approximately 0.66, with standard deviations between 0.2645 and 0.2741. The relatively wide ranges demonstrate meaningful variation across observations.

Table 13. Descriptive statistics of WGECR survival-probability features.

Feature	Mean	SD	Minimum	Median	Maximum
$S_{x_1}(t)$	0.6640	0.2645	0.0759	0.7416	0.9828
$S_{x_2}(t)$	0.6678	0.2722	0.0796	0.7427	0.9917
$S_{x_3}(t)$	0.6654	0.2741	0.1025	0.7527	0.9919
$S_{x_4}(t)$	0.6675	0.2696	0.0663	0.7580	0.9924
$S_{x_5}(t)$	0.6626	0.2684	0.0773	0.7551	0.9923

5.2.2. Relationship Between Original and Transformed Features

The relationship between each original predictor and its corresponding WGECR survival-probability feature was assessed using Pearson correlation. As shown in Table 14, the correlations were generally weak, ranging from −0.2200 to 0.1872. The strongest association was observed for $x_2(r = -0.2200)$, followed by $x_5(r = 0.1872)$ and $x_1(r = 0.1711)$. The correlations for x_3 and x_4 were close to zero.

Table 14. Correlation between original and WGECR-transformed features.

Feature	Correlation with $S_j(t)$.
x_1	0.1711
x_2	−0.2200
x_3	−0.0370
x_4	−0.0297
x_5	0.1872

The relatively weak association between the original predictors and their corresponding WGECR-derived survival features further supports the distinction between the two representations. If the transformation merely rescaled the original variables, we would generally expect a strong association between Xj and the transformed features. Instead, the transformed features represent the predictors through their estimated survival distributions. This indicates that the transformation is not simply a normalization procedure or a change in measurement scale. In the proposed Hybrid RSF, the combination of the two representations therefore provides the model with complementary forms of information: The original covariates preserve their observed characteristics, while the WGECR features provide a probabilistic survival-oriented representation.

5.2.3. Predictive Performance of the Proposed Hybrid RSF

The predictive performance of the three RSF configurations was assessed using C-index, IBS, and TD-AUC. The Hybrid RSF, which combines the original covariates with WGECR-derived survival-probability features, represents the primary proposed model. Conventional RSF and WGECR-RSF were included as comparative models to quantify the contribution of the WGECR transformation. The results are presented in Table 15.

Table 15. Predictive performance of the evaluated survival models.

Model	C-Index	IBS	TD-AUC
Original RSF	0.4286	0.2416	0.5901
WGECR-RSF	0.8697	0.0295	0.8799
Proposed Hybrid RSF	0.8798	0.0336	0.8862

The proposed Hybrid RSF achieved the highest C-index of 0.8798 and TD-AUC of 0.8862 among the three configurations, indicating superior overall discrimination and time-dependent classification performance. Although the WGECR-RSF obtained a slightly lower IBS of 0.0295, the Hybrid RSF retained the strongest discrimination and TD-AUC while incorporating both the original covariates and WGECR-derived survival-probability features. Compared with Conventional RSF, the proposed Hybrid RSF increased the C-index from 0.4286 to 0.8798 and TD-AUC from 0.5901 to 0.8862, while substantially reducing the IBS from 0.2416 to 0.0336. These findings support the Hybrid RSF as the principal proposed model, with the WGECR transformation providing additional distribution-informed information to the conventional covariate representation.

The three configurations provide a useful decomposition of the methodological contribution. Conventional RSF establishes the performance obtained from the original covariates alone, WGECR-RSF evaluates the predictive value of the distribution-derived representation independently, and the proposed Hybrid RSF combines both sources of information. This comparison demonstrates that the WGECR transformation provides substantial additional predictive information, while the Hybrid formulation further benefits from retaining the original covariates. The relatively small difference between the two WGECR-based configurations suggests that much of the predictive gain is associated with the distribution-informed representation, but the superior overall performance of the Hybrid RSF supports retaining both representations in the final model.

5.2.4. Cross-Validation Stability

The models were evaluated using five-fold cross-validation repeated five times, resulting in 25 valid evaluations. The mean C-index and standard deviation are presented in Table 16.

Table 16. Cross-validation performance.

Model	Mean C-Index	SD
Original RSF	0.4286	0.1244
WGECR-RSF	0.8697	0.0950
Proposed Hybrid RSF	0.8798	0.0962

The proposed Hybrid RSF achieved the highest mean C-index, indicating the strongest and most consistent discriminative performance across the repeated cross-validation evaluations. Its variability was also substantially lower than that of the Conventional RSF, with the SD declining from 0.1244 to 0.0962. The WGECR-RSF showed a similar level of stability, with a slightly lower SD of 0.0950. Above all, the results demonstrate that incorporating

WGECR-derived survival-probability features alongside the original covariates provides a stable predictive representation for the proposed Hybrid RSF. Figure 9 presents the fold-level C-index distributions using box plots, while the bootstrap confidence interval for the improvement of the proposed method is presented alongside the model comparison.

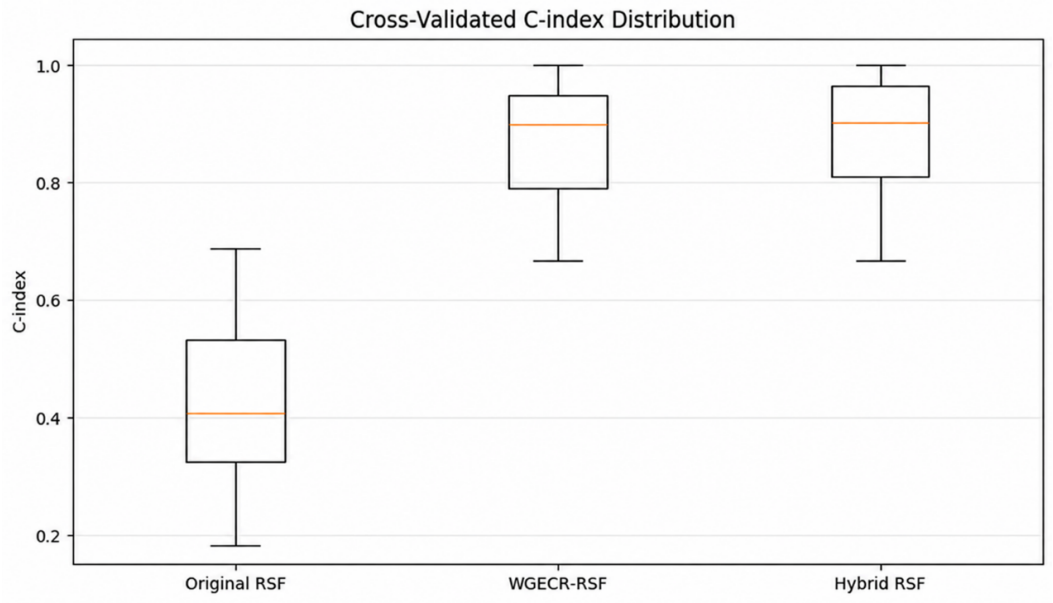


Figure 9. C-index box plot across folds.

5.2.5. Statistical Significance

The mean improvement in C-index of the Hybrid RSF over the original RSF was 0.4411 as presented in Table 17. The paired comparison produced a t-statistic of 11.6360 with $p < 0.001$. The Wilcoxon signed-rank test also indicated a statistically significant difference ($p < 0.001$). The bootstrap analysis yielded a 95% confidence interval of $[0.3693, 0.5105]$ for the mean improvement, which did not include zero.

Table 17. Statistical comparison between Original RSF and WGECR-$S(t)$-RSF.

Analysis	Statistic	Result
Mean C-index improvement	0.4411	—
Paired t-test	11.6360	$p < 0.001$
Wilcoxon signed-rank	0.0000	$p < 0.001$
Bootstrap 95% CI	[0.3693, 0.5105]	Excludes 0

The results provide consistent evidence of improved predictive performance for the Hybrid RSF relative to the original RSF.

5.2.6. Feature Importance

We assessed the contribution of the Hybrid RSF using permutation importance. As shown in Table 18 and Figure 10, $S_{x_3}(t)$ was the most influential transformed feature, followed by $S_{x_1}(t)$ and $S_{x_4}(t)$. $S_{x_2}(t)$ made a smaller contribution, whereas $S_{x_5}(t)$ showed negligible permutation importance.

The ranking indicates that the contribution of the distribution-derived features is not uniform. In particular, $S_{x_3}(t)$ provided the largest contribution to RSF prediction, whereas $S_{x_5}(t)$ contributed little under the permutation-based assessment.

Table 18. Permutation importance of WGECR survival-probability features.

Transformed Feature	Mean Importance	SD	Rank
$S_{x_3}(t)$	0.0526	0.0126	1
$S_{x_1}(t)$	0.0363	0.0101	2
$S_{x_4}(t)$	0.0323	0.0096	3
$S_{x_2}(t)$	0.0162	0.0102	4
$S_{x_5}(t)$	0.0001	0.0074	5

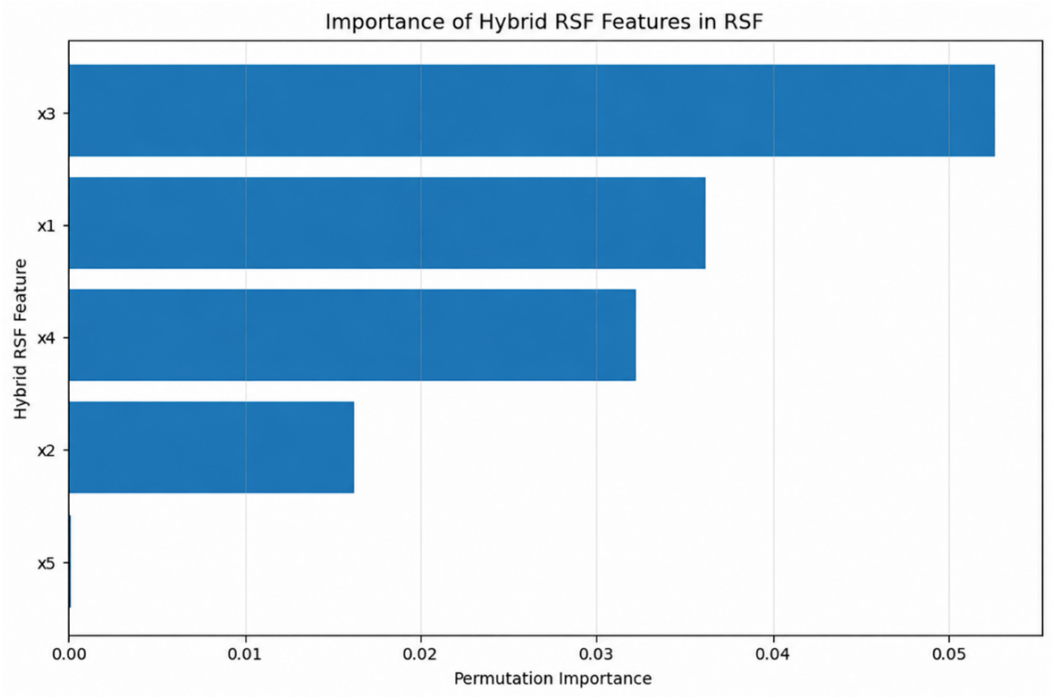


Figure 10. Permutation importance plot of WGECR-RSF.

The findings provide evidence that incorporating WGECR-derived survival-probability features alongside the original covariates can substantially enhance the predictive performance of RSF. The proposed Hybrid RSF achieved the strongest overall discrimination and time-dependent predictive performance among the evaluated configurations while retaining the original covariate information. Importantly, the improvement was achieved without modifying the underlying RSF algorithm; the methodological contribution occurs at the feature-representation level. The comparison with the WGECR-RSF further indicates that the WGECR-derived representation contributes substantial predictive information, while retaining the original covariates provides an additional, albeit relatively small, contribution. These findings support the proposed Hybrid RSF as the preferred formulation of the methodology.

Why Does WGECR Transformation Improve RSF?

A raw covariate and a survival-oriented representation convey information in fundamentally different forms. In Conventional RSF, predictors are supplied in their original measurement scales, leaving the forest to discover their relationships with survival through recursive partitioning. Although RSF can capture nonlinear associations, the raw numerical representation does not explicitly encode the probabilistic survival characteristics associated with a predictor. The WGECR transformation addresses this limitation by mapping each predictor to a conditional survival probability, $S_j(\tau \mid X_j)$. The resulting feature expresses the predictor in terms of its estimated relationship with survival rather than solely

through its original numerical magnitude. This provides RSF with an additional probabilistic representation that may facilitate the identification of survival-relevant patterns. In the proposed Hybrid RSF, this information is retained alongside the original covariates, allowing the forest to exploit both measurement-scale and distribution-informed representations. Thus, WGECR does not replace RSF or alter its learning mechanism; rather, it provides an additional statistical representation through which RSF can learn nonlinear interactions and generate the final survival predictions.

The proposed WGECR model proved to be useful in analyzing right-censored survival data in this study. The model is flexible and can be used to model different failure mechanisms competing with each other, and includes several distributional and reliability functions that can be of interest in survival and reliability analysis. The results obtained from the maximum likelihood analysis, combined with the model validation procedures, suggest that the model proposed is a good representation of the observed survival data. The WGECR model has the maximum LogL and the smallest values of AIC, AICc, and BIC in the fitted models for the Myeloma dataset. It also has the least Cox–Snell discrepancy, $D_{CS} = 0.2376$. The outcomes are always in favor of the proposed model as compared with the other distributions included in the analysis. The fitted WGECR survival function is very close to the Kaplan–Meier estimate, giving further graphical evidence of the suitability of the fitted model to the data. The parametric bootstrap analysis also confirms the numerical stability of the proposed model. All model fits were successful, based on 2,000 resamples of the model. The estimates of θ and λ from the bootstrap procedure were reasonably close to the maximum likelihood estimates, and the biases were relatively small. A higher variance in α was found, however, suggesting that caution is needed in analyzing this parameter. The analysis also revealed that the large variance in the estimates of α was primarily due to the relatively small number of extreme estimates in the central and extreme regions of the bootstrap distribution.

Several limitations should be considered when interpreting the findings. First, the Myeloma dataset is relatively small, which may affect the stability of WGECR parameter estimation and RSF predictions. Second, the analysis is based on a single dataset, limiting the generalizability of the findings to other populations and survival settings. Third, WGECR parameters are estimated numerically and may be sensitive to optimization settings and starting values. The selected prediction horizon may also influence the resulting survival-probability features and should therefore be specified carefully. Finally, although repeated cross-validation provides evidence of predictive stability within the available data, independent external validation using larger datasets is required to establish the robustness and general applicability of the proposed Hybrid RSF.

6. Conclusions

A new flexible right-censored survival analysis model, the WGECR model, was proposed. The distributional and reliability properties were determined, and maximum likelihood estimation, goodness-of-fit measures, and parametric bootstrap validation techniques were used for making statistical inferences. The WGECR model best fit the overall data for the Myeloma dataset for the models considered. The stability of the estimation procedure was confirmed by the bootstrap analysis, but a higher variability appeared in the estimation of the parameter α.

This study proposed a distribution-informed Hybrid RSF that integrates the original covariates with survival-probability features derived from the WGECR distribution. Unlike approaches that modify the internal structure of RSF, the proposed method preserves the conventional RSF learning mechanism while enriching its input representation with distribution-informed survival information. The comparative results demonstrate that the

proposed Hybrid RSF provides the strongest overall predictive performance among the evaluated configurations, achieving the highest C-index and TD-AUC. The feature-importance analysis further indicates that the contribution of the WGECR-informed representations is heterogeneous, with x_3, x_1, and x_4 emerging as the most influential features in the proposed model. Above all, the findings demonstrate the potential of using flexible probability distributions as survival-oriented feature representations and establish the proposed Hybrid RSF as a promising approach for integrating statistical distributional information with machine-learning survival prediction. Further validation on larger and independent survival datasets is required to establish its generalizability and practical applicability.

Future studies should also examine alternative parameter estimation strategies, the sensitivity of the model to prediction horizons, and the potential integration of additional clinical and demographic information.

Author Contributions: Conceptualization, A.U.U.; methodology, A.I.I. and A.U.U.; software, A.I.I. and A.U.U.; validation, A.I.I.; formal analysis, A.M.A.A. and A.F.I.A.; investigation, A.M.A.A. and A.F.I.A.; resources, A.M.A.A. and A.F.I.A.; data curation, A.I.I. and A.U.U.; writing—original draft preparation, A.M.A.A. and A.I.I.; writing—review and editing, A.I.I. and A.U.U.; visualization, A.I.I.; supervision, A.F.I.A.; project administration, A.I.I.; and funding acquisition, A.M.A.A. and A.F.I.A. All authors have read and agreed to the published version of the manuscript.

Funding: This research was funded by the Prince Sattam bin Abdulaziz University through the project number (PSAU/2026/03/41927).

Data Availability Statement: The dataset considered in this research is available in [23].

Acknowledgments: The authors extend their appreciation to Prince Sattam bin Abdulaziz University for funding this research through the project number (PSAU/2026/03/41927).

Conflicts of Interest: The authors declare no conflicts of interest.

References

1. Cox, D.R. Regression models and life-tables. *J. R. Stat. Soc. Ser. B (Methodol.)* **1972**, *34*, 187–202. https://doi.org/10.1111/j.2517-6161.1972.tb00899.x
2. Kalbfleisch, J.D.; Prentice, R.L. *The Statistical Analysis of Failure Time Data*, 2nd ed.; John Wiley & Sons: Hoboken, NJ, USA, 2002. https://doi.org/10.1002/9781118032985
3. Lawless, J.F. *Statistical Models and Methods for Lifetime Data*, 2nd ed.; Wiley-Interscience: Hoboken, NJ, USA, 2003. https://doi.org/10.1002/9781118033005
4. Prentice, R.L.; Kalbfleisch, J.D.; Peterson, A.V.; Flournoy, N.; Farewell, V.T.; Breslow, N.E. The analysis of failure times in the presence of competing risks. *Biometrics* **1978**, *34*, 541–554. https://doi.org/10.2307/2530374
5. Geskus, R.B. *Data Analysis with Competing Risks and Intermediate States*; Chapman & Hall/CRC: Boca Raton, FL, USA, 2015. https://doi.org/10.1201/b18695
6. Fine, J.P.; Gray, R.J. A proportional hazards model for the subdistribution of a competing risk. *J. Am. Stat. Assoc.* **1999**, *94*, 496–509. https://doi.org/10.1080/01621459.1999.10474144
7. Cox, D.R. The analysis of exponentially distributed life-times with two types of failure. *J. R. Stat. Soc. Ser. B (Methodol.)* **1959**, *21*, 411–421. https://doi.org/10.1111/j.2517-6161.1959.tb00349.x
8. Kalbfleisch, J.D.; Prentice, R.L. *The Statistical Analysis of Failure Time Data*; John Wiley & Sons: New York, NY, USA, 1980.
9. Gray, R.J. A class of *K*-sample tests for comparing the cumulative incidence of a competing risk. *Ann. Stat.* **1988**, *16*, 1141–1154. https://doi.org/10.1214/aos/1176350951
10. Elshahhat, A.; Nassar, M. Inference of improved adaptive progressively censored competing risks data for Weibull lifetime models. *Stat. Pap.* **2024**, *65*, 1163–1196. https://doi.org/10.1007/s00362-023-01417-0
11. Weibull, W. A statistical distribution function of wide applicability. *J. Appl. Mech.* **1951**, *18*, 293–297. https://doi.org/10.1115/1.4010337
12. Gupta, R.D.; Kundu, D. Theory & Methods: Generalized exponential distributions. *Aust. N. Z. J. Stat.* **1999**, *41*, 173–188. https://doi.org/10.1111/1467-842X.00072

13. Gupta, R.D.; Kundu, D. Generalized exponential distribution: Existing results and some recent developments. *J. Stat. Plan. Inference* **2007**, *137*, 3537–3547. https://doi.org/10.1016/j.jspi.2007.03.030
14. Alotaibi, R.; Rezk, H.; Park, C. Parameter estimation of inverse Weibull distribution under competing risks based on the expectation–maximization algorithm. *Qual. Reliab. Eng. Int.* **2024**, *40*, 3795–3808. https://doi.org/10.1002/qre.3599
15. Alhidairah, S.; Alam, F.M.A.; Nassar, M. A new competing risks model with applications to blood cancer data. *J. Radiat. Res. Appl. Sci.* **2024**, *17*, 101001. https://doi.org/10.1016/j.jrras.2024.101001
16. Sarhan, A.M.; Gomaa, R.S.; Magar, A.M.; Alsadat, N. Bivariate exponentiated generalized inverted exponential distribution with applications on dependent competing risks data. *AIMS Math.* **2024**, *9*, 29439–29473. https://doi.org/10.3934/math.20241427
17. Dimitrakopoulou, T.; Karagrigoriou, A.; Makrides, A.; Vonta, I. Competing risks modelling via multistate system methodology under a generalized family of distributions. *Methodol. Comput. Appl. Probab.* **2025**, *27*, 41. https://doi.org/10.1007/s11009-025-10169-3
18. Lindqvist, B.H. Phase-type models for competing risks, with emphasis on identifiability issues. *Lifetime Data Anal.* **2023**, *29*, 318–341. https://doi.org/10.1007/s10985-022-09547-7
19. Lo, S.M.S.; Wilke, R.A. A parametric competing risks regression model with unknown dependent censoring. *J. R. Stat. Soc. Ser. C Appl. Stat.* **2023**, *72*, 1079–1093. https://doi.org/10.1093/jrsssc/qlad042
20. Lo, S.M.S.; Wilke, R.A. A single risk approach to the semiparametric competing risks model with parametric Archimedean risk dependence. *J. Multivar. Anal.* **2024**, *201*, 105276. https://doi.org/10.1016/j.jmva.2023.105276
21. Monterrubio-Gómez, K.; Constantine-Cooke, N.; Vallejos, C.A. A review on statistical and machine learning competing risks methods. *Biometrical J.* **2024**, *66*, e2300060. https://doi.org/10.1002/bimj.202300060
22. Geskus, R.B. Competing risks: Concepts, methods, and software. *Annu. Rev. Stat. Appl.* **2024**, *11*, 227–254. https://doi.org/10.1146/annurev-statistics-040522-094556
23. Krall, J.M.; Uthoff, V.A.; Harley, J.B. A step-up procedure for selecting variables associated with survival. *Biometrics* **1975**, *31*, 49–57. https://doi.org/10.2307/2529709
24. Xie, M.; Lai, C.D. Reliability analysis using an additive Weibull model with bathtub-shaped failure rate function. *Reliab. Eng. Syst. Saf.* **1996**, *52*, 87–93. https://doi.org/10.1016/0951-8320(95)00149-2
25. El-Bassiouny, A.H.; El-Damcese, M.; Mustafa, A.; Eliwa, M.S. Exponentiated generalized Weibull-Gompertz distribution with application in survival analysis. *J. Stat. Appl. Probab.* **2017**, *6*, 7–16. https://doi.org/10.18576/jsap/060102
26. Abdullahi, U.A.; Liu, Y.; Qin, Y. Bayesian analysis of a flexible two-mode competing risk model using Hamiltonian Monte Carlo and applications to reliability datasets. *Commun. Stat. Theory Methods* **2026**, *55*, 4860–4884. https://doi.org/10.1080/03610926.2026.2624663
27. Sarhan, A.M.; Apaloo, J. Exponentiated modified Weibull extension distribution. *Reliab. Eng. Syst. Saf.* **2013**, *112*, 137–144. https://doi.org/10.1016/j.ress.2012.10.013
28. Marshall, A.W.; Olkin, I. A new method for adding a parameter to a family of distributions with application to the exponential and Weibull families. *Biometrika* **1997**, *84*, 641–652. https://doi.org/10.1093/biomet/84.3.641
29. Cox, D.R.; Snell, E.J. A general definition of residuals. *J. R. Stat. Soc. Ser. B (Methodol.)* **1968**, *30*, 248–265. https://doi.org/10.1111/j.2517-6161.1968.tb00724.x
30. Efron, B.; Tibshirani, R.J. *An Introduction to the Bootstrap*; Monographs on Statistics and Applied Probability, Volume 57; Chapman & Hall: New York, NY, USA, 1993. https://doi.org/10.1201/9780429246593
31. Daud, H.; Suleiman, A.A.; Ishaq, A.I.; Alsadat, N.; Elgarhy, M.; Usman, A.; Wiratchotisatian, P.; Ubale, U.A.; Liping, Y. A new extension of the Gumbel distribution with biomedical data analysis. *J. Radiat. Res. Appl. Sci.* **2024**, *17*, 101055. https://doi.org/10.1016/j.jrras.2024.101055
32. Ishwaran, H.; Kogalur, U.B.; Blackstone, E.H.; Lauer, M.S. Random survival forests. *Ann. Appl. Stat.* **2008**, *2*, 841–860. https://doi.org/10.1214/08-AOAS169
33. Panitanarak, U.; Ishaq, A.I.; Sawaran Singh, N.S.; Usman, A.; Usman, A.U.; Daud, H.; Adepoju, A.A.; Sadiq, I.A.; Suleiman, A.A. Machine learning models in predicting failure times data using a novel version of the Maxwell model. *Eur. J. Stat.* **2025**, *5*, 1. https://doi.org/10.28924/ada/stat.5.1
34. Wiegrebe, S.; Kopper, P.; Sonabend, R.; Bischl, B.; Bender, A. Deep learning for survival analysis: A review. *Artif. Intell. Rev.* **2024**, *57*, 65. https://doi.org/10.1007/s10462-023-10681-3
35. Zhao, B.; Nguyen, V.K.; Xu, M.; Colacino, J.A.; Jolliet, O. Random survival forest for predicting the combined effects of multiple physiological risk factors on all-cause mortality. *Sci. Rep.* **2024**, *14*, 15566. https://doi.org/10.1038/s41598-024-66261-0
36. Loffredo, G.; Romano, E.; Maturo, F. Random survival forest for censored functional data. *Stat. Med.* **2025**, *44*, e10344. https://doi.org/10.1002/sim.10344
37. Garcia-Lopez, A.; Jiménez-Gómez, M.; Gomez-Montero, A.; Gonzalez-Sierra, J.C.; Cabas, S.; Giron-Luque, F. Survival analysis using machine learning in transplantation: A practical introduction. *BMC Med. Inform. Decis. Mak.* **2025**, *25*, 141. https://doi.org/10.1186/s12911-025-02951-7

38. Ishag, M.A.S.; Wanjoya, A.; Adem, A.; Alsultan, R.; Alghamdi, A.S.; Afify, A.Z. The exponentiated-Weibull proportional hazard regression model with application to censored survival data. *Alex. Eng. J.* **2024**, *104*, 587–602. https://doi.org/10.1016/j.aej.2024.08.007
39. Ameeq, M.; Naz, S.; Tahir, M.; Hassan, M.M.; Jamal, F.; Fatima, L.; Shahzadi, R. A new Marshall-Olkin Lomax distribution with application using failure and insurance data. *Statistics* **2024**, *58*, 450–472. https://doi.org/10.1080/02331888.2024.2341792
40. Ishaq, A.I.; Usman, A.U.; Alqifari, H.N.; Almohaimeed, A.; Daud, H.; Abba, S.I.; Suleiman, A.A. A new Log-Lomax distribution, properties, stock price, and heart attack predictions using machine learning techniques. *AIMS Math.* **2025**, *10*, 12761–12807. https://doi.org/10.3934/math.2025575

Disclaimer/Publisher's Note: The statements, opinions and data contained in all publications are solely those of the individual author(s) and contributor(s) and not of MDPI and/or the editor(s). MDPI and/or the editor(s) disclaim responsibility for any injury to people or property resulting from any ideas, methods, instructions or products referred to in the content.